RESEARCH ACTIVITIES IV
Department of Molecular Assemblies

IV-A Spectroscopic Study of Charge Carriers in Organic Conductors

The low-frequency reflectivity of an organic conductor provides us with a wealth of information on the nature of charge carriers. For instance, the anisotropy of a band structure, bandwidth, effect of electron-electron correlation, and electron-molecular vibration (*e-mv*) coupling parameters can be extracted from the analysis of the reflectivity or optical conductivity curve. We are investigating the polarized reflection spectra of various organic conductors in the spectral region of 50–33000 cm^{-1} and in the temperature range of 6–300 K. Usually the molecular vibrations (local phonons) are screened by strong electronic transition by charge carriers. Therefore, few local phonon bands are detected in the reflection spectrum. In this sense, the Raman spectroscopy is a complementary method to reflection spectroscopy for understanding molecular vibrations in a metallic state. Since some molecules have charge-sensitive vibrational modes, the Raman spectroscopic method is a powerful tool to detect the site-charge distribution (oxidation state of molecule). We are investigating the charge ordering (CO) phenomena in organic conductors using the technique of infrared and Raman spectroscopy. In the organic charge-transfer salts, CO is originated from the localization of the charge carriers. Since the charge carriers in organic crystal is located at the boundary between localized and extended (delocalized) states, CO will be widely found through the phase transition. The charge ordering was first found in inorganic narrow-band systems such as copper, manganese, and vanadium oxides. Recently, CO has been found in several organic conductors, and the electronic phase diagrams of typical organic conductors are re-examined taking CO into account. The CO state is drawing attention, since CO is theoretically considered as being related to the pairing mechanism in superconductivity. The Raman and infrared spectra change dramatically at the CO phase-transition temperature, since CO is accompanied by an inhomogeneous charge distribution. Our goal is the complete understanding of the CO phase transition through the interpretation of the vibrational spectra, and the drawing of a *P-T* phase diagram.

IV-A-1 Infrared and Raman Evidence for the Charge Ordering in β”-(BEDT-TTF)$_3$(ReO_4)$_2$ Studied by Vibrational Spectroscopy

YAMAMOTO, Takashi; URUICHI, Mikio; YAKUSHI, Kyuya; YAMAURA, Jun-ichi[1]; TAJIMA, Hiroyuki[1]
([1]Univ. Tokyo)

[*Phys. Rev. B* in press]

The charge-ordering (CO) state is drawing attention as a new electronic ground state in narrow-band organic charge-transfer salts which do not have a strong dimer unit. The mechanism of the metal-insulator transition of β”-type ET salts (ET = bis-ethylenedithio-tetrathia-fulvalene) has not been understood well. As the first step to investigate the ground state of β”-type ET salts, we started from the 3:2 salts, where the carrier density is higher than those of the 2:1 salts. The infrared and Raman spectra of β”-$(ET)_3(ReO_4)_2$ were measured at various temperatures below 300 K. We investigated the three C=C stretching modes, ν_2, ν_{27} and ν_3. The infrared and Raman spectra discontinuously changed at 80 K. Below 80 K, for example, the doublet ν_2 bands split into three peaks, the doublet ν_{27} also split into three, and a mutual exclusion rule for the vibronic ν_3 modes in the infrared and Raman spectra is broken. This symmetry lowering is consistent with the result of x-ray crystal structure analyses conducted at 100 K and 22 K. The site charges in the unit cell estimated from the splitting of ν_2 are $+0.7_3$, $+0.7_3$, and $+0.5_3$ in the metallic phase above 81 K, and they are changed into +0.2, $+0.8_5$, and $+0.9_5$ in the insulating phase below 80 K. The pattern of the site charge distributions exhibits the re-distribution at 80 K, which is shown in the figures. The frequencies of the vibronic ν_3 modes are reproduced from the numerical calculation by assuming of the patterns in the figures. From these experimental results, the metal-insulator transition of this compound is characterized as the CO transition originated from the localization of charge due to Coulomb interactions.

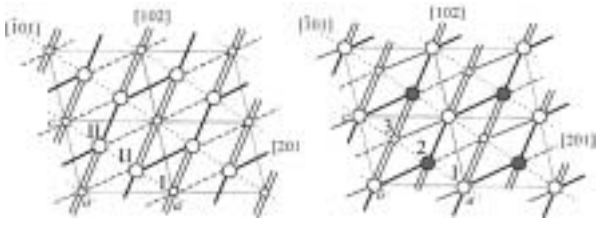

Figure 1. The site charge distributions above 81 K (left) and below 80 K (right). The symbols, ○ and ○ in the left denote the site charges of 0.7_3 and 0.5_3, and the symbols ○, ●, and ○ denote the site charges of 0.9_5, 0.8_5, and 0.2. The lines represent the magnitude of transfer integrals, which is schematically shown as follows: double > single > dashed > dotted.

IV-A-2 Charge Ordering State of β”-(ET)$_3$(HSO_4)$_2$ and β”-(ET)$_3$(ClO_4)$_2$

YAMAMOTO, Takashi; URUICHI, Mikio;

YAKUSHI, Kyuya; KAWAMOTO, Atsushi[1]
([1]Hokkaido Univ.)

In the previous study, we have demonstrated the charge-ordering (CO) phase transition of β"-$(ET)_3(ReO_4)_2$ at 80 K. However, this CO phase transition is accompanied by a drastic structural change. On the other hand, no remarkable structural change is observed in the metal-insulator transition of β"-$(ET)_3(HSO_4)$ and β"-$(ET)_3(ClO_4)$ salts. This enables us to discuss purely the role of the inter-site Coulomb repulsion, *V*, in the CO state. The Raman and IR spectra of β"-$(ET)_3X_2$ (X = HSO_4 and ClO_4) were measured at various temperatures below 300 K. We investigated three C=C stretching modes, namely ν_2, ν_3 and ν_{27}. The spectral patterns of both compounds in the low temperature phases are ascribed to the CO state, where the site charges at charge-poor and charge-rich sites are $\sim+0.3_3$ and $\sim+0.8_3$. The pattern of the CO state in X = HSO_4 salt is identical to that in X = ClO_4 salt but differs from that of X = ReO_4 salt. We have found that the patterns of the CO states are correlated with the inter-molecular distances between the centers of adjacent molecules along the stacking direction. Since the intermolecular distance at the non-slipping point is shorter than that at the slipping point, *V* at the non-slipping point is larger than that at the slipping point. The unit cells of X = HSO_4 and ClO_4 salts contain two non-slipping points whereas an organic layer of the unit cell of X = ReO_4 salt contains one non-slipping point. This structural difference explains the difference in the CO pattern. Through the analyses of the experimental results, we have demonstrated direct evidence for the role of the inter-site Coulomb repulsion in the CO state.

IV-A-3 Inhomogeneous Charge Distributions in β"-$(ET)_4Ga(C_2O_4)_3$sol (sol = $PhNO_2$, Py and Ch_2Cl_2)

YAMAMOTO, Takashi; URUICHI, Mikio; YAKUSHI, Kyuya; AKUTSU, Hiroki[1]; SATO-AKUTSU, Akane[1]; DAY, Peter[2]
([1]Himeji Inst. Tech.; [2]Royal Inst. GB)

The reason for the strong attention to the charge ordering (CO) is the theoretical prediction that the superconducting (SC) state neighbored on the CO state has a new paring mechanism. Among various non-dimerized ET salts, the β"-type ET salts have attracted attention, because the superconductivity has been found in various β"-type ET salts under hydrostatic pressure. The most interesting point of the title compounds is that they demonstrate superconductivity at ambient pressure. According to the resistivity measurements of the title compounds, the metal-insulator transitions are observed at around 100 K. The electrical resistivity of solvent = Py (pyridine) and CH_2Cl_2 salts keep the insulating behavior down to the liquid-helium temperature. On the other hand, the insulator-superconductor transition is observed at 7.5 K in the electrical resistivity of solvent = $PhNO_2$ (nitrobenzene) salt. The conducting behavior of the title compounds is unique since the SC phase appears with increasing the volume of the unit cell. We have tentatively measured the Raman and IR spectra of these compounds down to 13 K. The ν_{27} and ν_2 modes have the broad line-widths around 300 K. With decreasing temperature, these modes show the peak splitting, suggesting the CO state. The difference in the site charge distributions, $\Delta\rho$, has the large value with increasing the size of the solvent molecule in the crystal. The reflectivity in the infrared region decreases as the size of the solvent molecule increases. Our observations suggest the view that that the SC phase is neighbored on the CO phase.

IV-A-4 Infrared and Raman Study of the Charge-Ordered State of θ-$(ET)_2Cu_2CN[N(CN)_2]_2$

YAMAMOTO, Takashi; YAKUSHI, Kyuya; SHIMIZU, Hiroyasu[1]; SAITO, Gunzi[1]
([1]Kyoto Univ.)

[*J. Phys. Soc. Jpn.* **73**, 2326 (2004)]

According to the resistivity measurements of the θ-type ET salts, the conducting behavior can be mapped with the structural parameter, namely the dihedral angle, ϕ, which is defined from the adjacent molecules along the highly conducting direction. The title compound has the largest ϕ among the θ-type ET salts, and the electrical resistivity exhibits an insulating behavior even at 300 K. In order to clarify the electronic state of θ-type ET salts, the polarized Raman and infrared spectra of θ-$(ET)_2Cu_2CN[N(CN)_2]_2$ were measured at various temperatures below 300 K. We investigated the three C=C stretching modes, ν_2, ν_3 and ν_{27}. The spectral pattern below the phase transition temperature, ~220 K, is compatible with the horizontally charge-ordered state, where the site-charge distributions are $+0.1_7$ and $+0.8_3$. We have found that the vibronic ν_3 bands correlate to the dihedral angles, ϕ. This relation is well reproduced from the numerical calculation based on the cluster model with C_2 symmetry. Among four independent ν_3 bands, the lowest-frequency vibronic band is the most sensitive to ϕ. With increasing ϕ, the frequency of the vibronic band is elevated due to the decrease of the transfer integral (and increasing the magnitude of the Coulomb repulsions).

The spectral features above the phase transition temperature, ~220 K, also exhibit the peak splitting due to the precursory effect of the CO state. The charges are nearly localized, and perhaps the short-range ordered horizontal CO stripe is dynamically fluctuating in the high-temperature phase above 220 K.

IV-A-5 Re-Examination of the Charge Sensitive Vibrational Modes in ET Molecule

YAMAMOTO, Takashi; YAKUSHI, Kyuya; URUICHI, Mikio; YAMAMOTO, Kaoru; KAWAMOTO, Atsushi[1]; TANIGUCHI, Hiromi[2]
([1]Hokkaido Univ.; [2]Saitama Univ.)

The phase transition from charge-ordering (CO) phase to superconducting (SC) phase has not been experimentally observed. Such an experiment will be able to be conducted in the β"-type ET salts using

vibrational spectroscopic method. However, the Raman technique is inappropriate, because the control of the sample temperature is difficult owing to the heating effect by the excitation lasers. On the other hand, the infrared reflectance technique enables us to measure the vibrational mode around the liquid helium temperature. Among the IR-active modes of the ET molecule, the ν_{27} mode is the candidate of the charge sensitive probe. We can expect that the frequency decreases with increasing the site charges. However, the relation between the frequency and the degree of the charge transfer is not well established. We detected the frequency of the ν_{27} mode of ET^+ through the measurement of the IR reflectance spectra of $(ET)(ClO_4)$, $(ET)(AuBr_2Cl_2)$ and the isotope analogues of $(ET)(AuBr_2Cl_2)$. The decided frequency is ~ 1400 cm^{-1}, which is remarkably different from 1445 cm^{-1} in the previous reports.

The frequency of the ν_{27} mode in the neutral ET crystal is lower than that of the charge-poor site of θ-$(ET)_2Cu_2CN[N(CN)_2]_2$ in the CO state. This contradictory result seems to be ascribed to the fact that the ET molecule in the neutral crystal has a boat structure and those of the charge transfer (CT) salts have a flat structure regardless of the degree of the charge transfer, ρ. This conjecture was verified from the normal mode analysis using the DFT method: the frequency of ν_{27} in boat ET^0 is lower than that of flat ET^0. On the basis of our experimental results and calculations, we deduced the frequency shift of ν_{27} as $\Delta\nu$ ~ 135 cm^{-1}/e. The ν_{27} mode is the efficient probe to the site charges in the ET salts. Finally, we should emphasize that ν_{27} is free from *emv* effect and thus the frequency shift is directly related to the site charge.

IV-A-6 Suppression of the Charge Disproportionation by Hydrostatic Pressure in β”-(ET)(TCNQ)

URUICHI, Mikio; YAKUSHI, Kyuya; YAMAMOTO, Hiroshi[1,2]; KATO, Reizo[1,2]
([1]RIKEN; [2]JST-CREST)

Charge disproportionation (CD) and charge ordering (CO) in organic conductors originate from the localization of charge carriers. CO has been investigated in the insulating states of several charge-transfer salts. Last year, we presented dynamically fluctuating CD in the metal-like state of the title compound. We measured the polarized Raman and infrared spectra. First we estimated the charge-transfer degree from ET to TCNQ as 0.5 using the C=C stretching mode (ν_4) of TCNQ. All of the Raman bands of TCNQ are independent of temperature. However, the C=C stretching modes (ν_2 and ν_3) of BEDT-TTF show clear splitting, and the low-frequency component of ν_3 exhibits a broad vibronic feature. This finding indicates that the holes of BEDT-TTF are nearly localized, and thus CD arises near the room temperature. Very interestingly, the split bands of ν_2 merge into a single broad band, and the broad band is sharpened on lowering temperature. The same phenomenon is found in the infrared-active C=C stretching mode ν_{27}. This temperature dependence is well reproduced by motional narrowing model. We interpreted this phenomenon as follows: The lowering the temperature contracts the crystal lattice and increases the transfer integral between the adjacent ET molecules. The slight enhancement of the transfer integral accelerates the hopping speed and causes the merge of the split band.

This compound consists of a segregated stack structure, where BEDT-TTF and TCNQ separately form uniform chains. We found week satellite reflections of $0.5a^* + 0.5c^*$ on X-ray diffraction patterns exposed for 8 hours. This result and the vibronic band of infrared spectra polarized to TCNQ stack direction are consistent with dimerization of TCNQ. This year, we applied the hydrostatic pressure to contract the crystal lattice. The split bands of ν_2 again merge into a single broad band, and the broad band is sharpened on increasing pressure. All of the Raman bands of TCNQ are independent of pressure. The same phenomenon is found in the temperature dependence of Raman spectra.[1)]

Reference

1) K. Yakushi, M. Uruichi, H. M. Yamamoto and R. Kato, *J. Phys. IV France* **114**, 149–151 (2004).

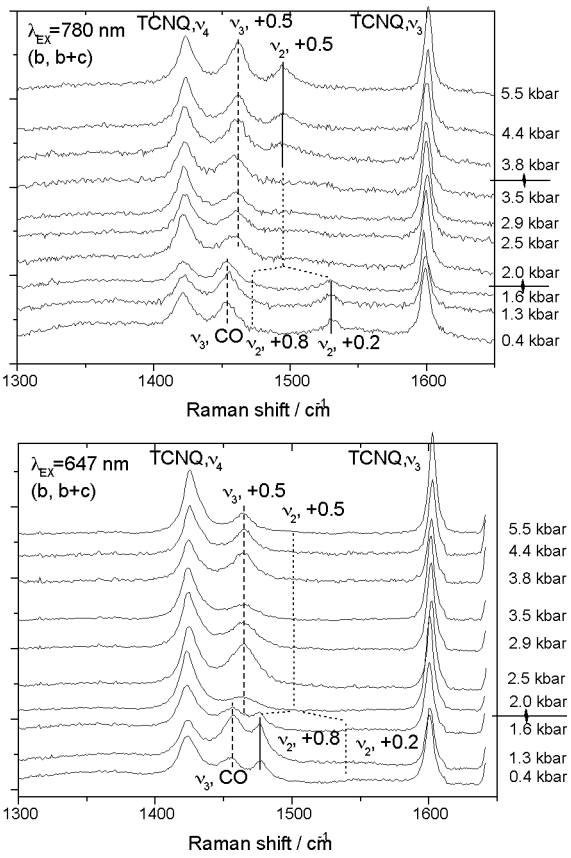

Figure 1. Pressure dependence of the Raman spectra of β”-(ET)(TCNQ) at room temperature.

IV-A-7 Electron-Molecular Vibration Coupling Effect on the Raman Spectrum of Organic Charge Transfer Salts

YAMAMOTO, Kaoru; YAKUSHI, Kyuya

[*J. Phys. IV France* **114**, 153 (2004)]

Vibrational spectra of dimerized and tetramerized radical clusters have been calculated to understand the features of electron-molecular vibration (EMV) coupling effects for the charge ordered (CO) system. The calculated spectra show that the totally in-phase Raman band, which is usually used as a measure of the molecular ionicity, approaches to the frequency corresponding to the average molecular ionicity in the cluster, as we increase the EMV coupling constant. When the charge disproportionation (CD) ratio is not large, the frequency of this mode is independent of the molecular ionicity. On the other hand, when large CD presents, the in-phase Raman bands show steep shift for small variation of the CD ratio. These results suggest that concerning to the normal modes with a large EMV coupling constant, we should not use the Raman-active band to estimate the molecular ionicity. We should use the Raman-active mode with small EMV coupling constant or infrared-active mode for the estimation of the molecular ionicity.

IV-A-8 Activation of Strong Overtone in the Infrared Spectrum of a Charge Ordered Organic Conductor

YAMAMOTO, Kaoru; YAKUSHI, Kyuya

Activation of overtones (OT) (asterisk in Figure 1) in the IR spectrum of θ-(BEDT-TTF)$_2$RbZn(SCN)$_4$ has been investigated using a diatomic molecular dimer model. When the two molecules are in the charge disproportionation for some reason, deformation of the two molecules along the anti-phase mode ($Q_- = Q_1 - Q_2$; $Q_{1,2}$: normal coordinates of molecule 1 and 2) stabilizes the disproportionation *via* electron-molecular vibration (EMV) coupling effect. This stabilization turns the electronic wavefunction (Ψ) to be dependent on Q_- and induces an unharmonicity in the vibronic energy,

$$\int \Psi^*(n_1 - n_2)Q_-\Psi dr$$

($n_{1,2}$: electron density on the molecule 1 and 2). Taking the Q_- dependence into account, we have calculated the optical conductivity spectrum including one totally symmetric C=C stretching mode (ν_3) using several fitting parameters, such as the vibronic coupling constants and the phenomenological site-energy difference. As shown by the dashed curve in Figure 1, the calculated spectrum reproduces the characteristics of the experimental data including the fundamental and overtone of ν_3. According to the model developed here, the overtone is only visible when the degree of charge disproportionation is large, and thus the emergence of overtone can be referred as evidence for the large charge disproportionation.

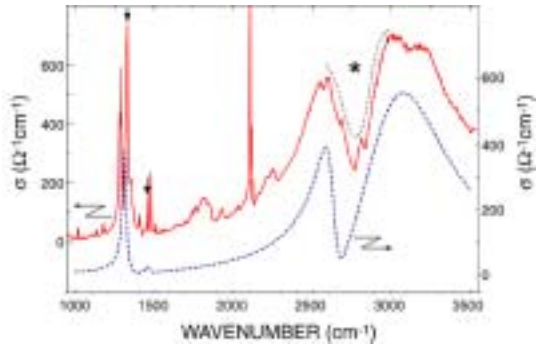

Figure 1. Solid curve shows the optical conductivity spectrum (E_{ph}//c-axis) of θ-(BEDT-TTF)$_2$RbZn(SCN)$_4$ measured at 50 K. Arrows and an asterisk indicate the fundamental and overtone of ν_3, respectively. The dashed curve shows the calculation results.

IV-A-9 Bond and Charge Density Waves in the Charge Localized Phase of (DI-DCNQI)$_2$Ag Studied by Single-Crystal Infrared and Raman Spectroscopy

YAMAMOTO, Kaoru; YAMAMOTO, Takashi; YAKUSHI, Kyuya; PECILE, Cesare[1]; MENEGHETTI, Moreno[1]
([1]Univ. Padova)

[*Phys. Rev. B* submitted]

The charge distribution and molecular arrangement of a 1/4-filled quasi-1D system (DI-DCNQI)$_2$Ag (DI-DCNQI = 2,5-diiodo-dicyanoquinediimine) have been studied by IR and Raman spectroscopy. The charge localization of this material was believed to be a 1D generalization of a Wigner crystal driven by inter-site Coulomb repulsion. While charge disproportionation (CD) is confirmed *via* the splitting of b_u modes in the infrared (IR) spectrum, the appearance of intense IR vibronic bands of a_g modes strongly suggests the presence of the dimerization that is not expected from the proposed 1010 charge ordering (CO) model (Wigner crystal). In addition, the selection rules for the IR and Raman signals cannot be explained without a further symmetry reduction of the unit cell. To explain the vibrational behavior observed for a single crystal, we show that a more appropriate model for the charge ordering is 0110 ($2k_F$ CDW + $4k_F$ BOW).

IV-A-10 Infrared and Raman Studies of TTM-TTP and TSM-TTP Charge-Transfer Salts

SWIETLIK, Roman[1]; YAKUSHI, Kyuya; YAMAMOTO, Kaoru; KAWAMOTO, Tadashi[2]; MORI, Takehiko[2]
([1]IMS and Inst. Molecular Phys.; [2]Tokyo Inst. Tech.)

The bis-fused TTF (tetrathiafulvalene) molecule and its derivatives are good electron donors for synthesis of new conducting ion-radical salts. One of these derivatives, TTM-TTF (see Figure 1) yields mostly quasi-one-dimensional semiconductors, because four S-CH$_3$ groups attached to the bis-fused TTF skeleton separate efficiently neighboring TTM-TTP stacks. Nevertheless,

some TTM-TTP salts exhibit metallic properties. The charge-transfer salt, (TTM-TTP)I_3 was reported as the first organic metal with 1:1 stoichiometry and a highly one-dimensional half-filled band. To investigate the relation between the molecular ionicity and the frequency of characteristic vibrational modes of TTM-TTP molecule, we measured room-temperature infrared and Raman spectra of neutral TTM-TTP molecule and four conducting charge-transfer salts with different molecular ionicity: (TTM-TTP)I_3, (TTM-TTP)AuI_3, (TTM-TTP)$(I_3)_{5/3}$, and (TSM-TTP)$(I_3)_{5/3}$. The vibrational bands related to the C=C stretching modes were analyzed. The frequencies of C=C stretching modes observed both in infrared and Raman spectra depend linearly upon the charge on TTM-TTP (or TSM-TTP) molecules.

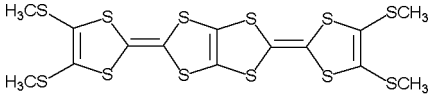

TTM-TTP

Figure 1. Structural formula of TTM-TTP.

IV-B Magnetic Resonance Studies for Molecular-Based Conductors

Magnetic resonance measurements are powerful investigations to understand the fundamental electronic properties, because they are microscopic and also dynamical measurements. Molecular based conductors are one of the extensively studied materials. The development of the understanding of the electronic phases of these materials enables us systematic investigations of low-dimensional highly correlated electrons systems. Competition of the electronic phases in molecular based conductors has attracted much attention. The investigations of such electronic phases by means of magnetic resonance measurements are important to understand the unsolved fundamental problems in the field of solid state physics.

In this project, we performed the multi-frequency ESR (X-, Q- and W-bands), and broad-line NMR measurements for molecular based conductors to understand the electron spin dynamics in the low temperature electronic phases.

IV-B-1 Competition Electronic States of $(TMTTF)_2MF_6$: ESR Investigations

NAKAMURA, Toshikazu; MAEDA, Keisuke[1]
([1]GUAS)

[*J. Phys. IV France* **114**, 123–124 (2004)]

ESR measurements were performed to investigate the low-temperature electronic states of $(TMTTF)_2MF_6$ (M = P, As, Sb and their mixed alloys). The temperature dependence of the ESR linewidth, ΔH_{pp}, of AsF_6 does not change its anisotropy at around T_{sp}. On the other hand, PF_6 and some P-AsF_6 alloys show changes of the ΔH_{pp} anisotropy at around T_{sp}, suggesting reconstruction of electronic charges. We propose the possible charge ordering configuration in the vicinity of the low temperature ground states from the ESR point of view.

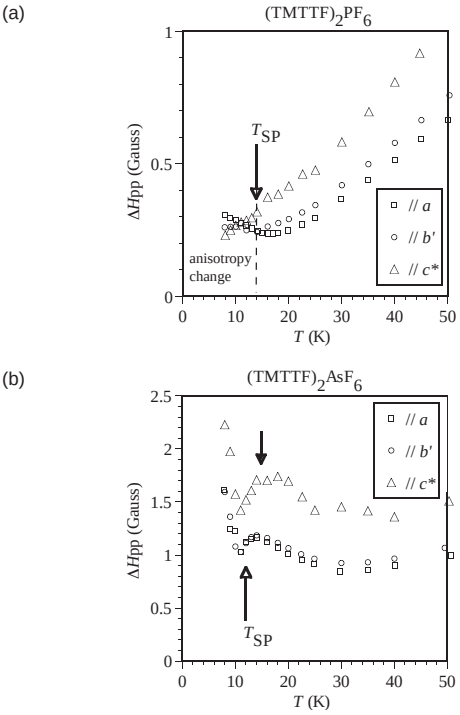

Figure 1. (a)–(b) Temperature dependence of the linewidth, ΔH_{pp}, for (a) PF_6 and (b) AsF_6 in the vicinity of the sP transitions.

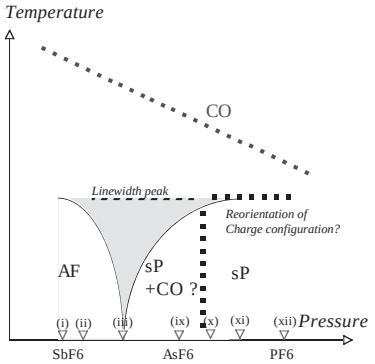

Figure 2. Schematic diagram of the possible electronic phases with the compositions (chemical pressures) for the MF_6 and their alloys deduced by the ESR results; (i)SbF_6, (ii) $(AsF_6)_{0.2}(SbF_6)_{0.8}$, (iii) $(AsF_6)_{0.5}(SbF_6)_{0.5}$, (ix) AsF_6, (x) $(PF_6)_{0.3}(AsF_6)_{0.7}$ (xi) $(PF_6)_{0.6}(AsF_6)_{0.4}$ and (xii) PF_6.

IV-B-2 ESR Study on Low-Dimensional Antiferromagnet α-$(BEDT\text{-}TTF)_2PF_6$ and ζ-$(BEDT\text{-}TTF)_2PF_6(THF)$

MAEDA, Keisuke[1]; HARA, Toshifumi; NAKAMURA, Toshikazu
([1]GUAS)

ESR measurements were carried out for α-$(BEDT\text{-}TTF)_2PF_6$ and ζ-$(BEDT\text{-}TTF)_2PF_6(THF)$. The temperature dependences of the spin susceptibility of the two salts are very similar to each other and seem to behave as typical paramagnetic insulators with low-dimensional antiferromagnetic interaction. The absolute values of the macroscopic antiferromagnetic interaction, J/k_B, are also very close. However, there are obvious differences in their ground states and microscopic behaviours. ζ-$(BEDT\text{-}TTF)_2PF_6(THF)$ undergoes an antiferromagnetic transition at around 5 K, while α-$(BEDT\text{-}TTF)_2PF_6$ shows no long-range magnetic ordering down to 2 K. The temperature dependent behaviours of the ESR linewidth, ΔH_{pp}, are quite different: The ΔH_{pp} of ζ-$(BEDT\text{-}TTF)_2PF_6(THF)$ is almost temperature independent in the paramagnetic region and shows an abrupt increase below about 30 K, while the ΔH_{pp} of α-$(BEDT\text{-}TTF)_2PF_6$ gradually decreases as the temperature decreases. The low temperature electronic states of these salts are discussed from the microscopic point of view.

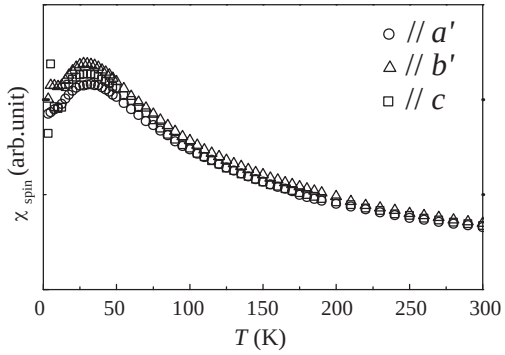

Figure 1. Temperature dependence of the spin susceptibility of α-(BEDT-TTF)$_2$PF$_6$. The exchange interaction, J/k_B, is about 27 K evaluated from the Bonner-Fisher model. This behavior is in good agreement with the static susceptibility measured by SQUID.

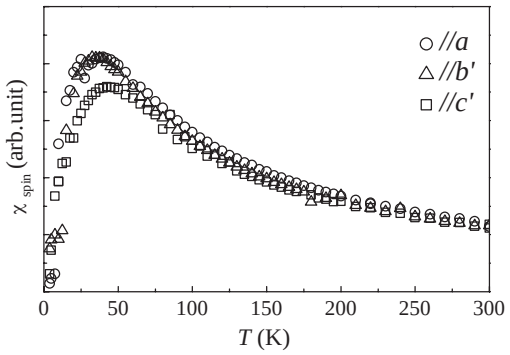

Figure 2. Temperature dependences of the spin susceptibility of ζ-(BEDT-TTF)$_2$PF$_6$(THF). The exchange interaction, J/k_B, is about 25 K.

IV-B-3 Multi-Frequency ESR Measurements for (TMTTF)$_2$*X*

HARA, Toshifumi; FURUKAWA, Ko; NAKAMURA, Toshikazu

TMTTF family salts are now attracted attention by the recent progress of the charge ordering (CO) investigations. Recently, we proposed the possible charge ordering configurations for each of (TMTTF)$_2$*X* salts according to the difference of the ESR linewidth anisotropy at low temperatures. The CO configurations of (TMTTF)$_2$*X* are roughly divided into three groups, and this classification is consistent with the results determined by other measurements. However the origin of the charge ordering phenomena is not clarified, and the quantitative understanding of the ESR linewidth is not succeeded so far. So we performed multi-frequency (X- [10 GHz], Q- [30 GHz], and W-bands [100 GHz]) ESR measurements for one of typical TMTTF salts, (TMTTF)$_2$SbF$_6$, which shows the charge ordering transition at 154 K. The ESR linewidth determined by the W-band measurement is obviously larger than that by X-band below the charge ordering transition. We discuss the low temperature electron spin dynamics from the ESR point of view.

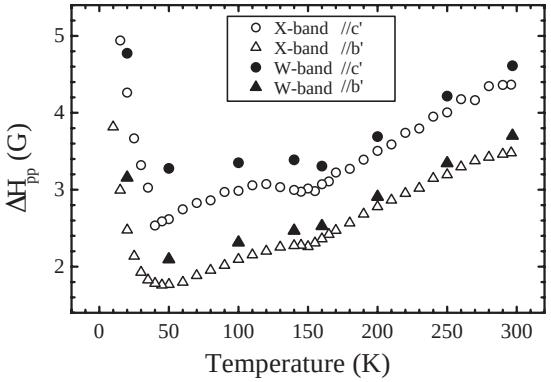

Figure 1. Temperature dependence of the ESR width, ΔH_{pp}, of (TMTTF)$_2$SbF$_6$ determined by X- (open symbols) and W-bands (solid symbols).

IV-B-4 Correlation between Molecular and Spin Structures of (TMTTF)$_2$*X*

FURUKAWA, Ko; HARA, Toshifumi; NAKAMURA, Toshikazu

The *g*-values of organic conductors are determined by the *g*-tensor of the radicals and their configuration. So the *g*-values of the crystal generally do not change with temperature. According our recent detailed ESR measurement, the *g*-values of the several TMTTF salts shows significant change with temperature, although these salts do not indicate structural changes. In order to understand the anomalous *g*-shift, we performed molecular orbital calculation with the Gaussian03, and estimated the *g*-values by the GIAO method. According to the calculation results, we found that the deformation of the TMTTF molecules along the molecular long axis cause a *g*-shift toward to an uni-axial symmetry. We can explain the anomalous *g*-shift observed if we assume the shrink of the TMTTF molecules along the molecular long-axis as the temperature decreases. Further structural investigation such as low-temperature X-ray measurements are now going on.

IV-B-5 Dynamical Charge Disproportionation in Metallic State in θ-(BEDT-TTF)$_2$RbZn(SCN)$_4$

TAKAHASHI, Toshihiro[1]; CHIBA, Ryo[1]; HIRAKI, Ko-ichi[1]; YAMAMOTO, M. Hiroshi[2]; NAKAMURA, Toshikazu
([1]Gakushuin Univ.; [2]Inst. Phys. Chem. Res.)

[*J. Phys. IV France* **114**, 269–272 (2004)]

Results of ^{13}C-NMR experiments on charge ordering in non-dimerized BEDT-TTF salts are discussed. It has been experimentally confirmed in θ-(ET)$_2$RbZn(SCN)$_4$ that charge disproportionation already develops well above the metal-insulator transition temperature while no long-range charge order is stabilized. Dynamics of the charge fluctuations has been determined in this salt and compared with the situations in α-(ET)$_2$I$_3$. This result seems to require a serious reconsideration of the transport properties in the metallic state.

IV-B-6 Charge Disproportionation in the Metallic States of α-(BEDT-TTF)$_2$I$_3$

MOROTO, Shiori[1]; HIRAKI, Ko-ichi[1]; TAKANO, Yoshiki[1]; TAKAHASHI, Toshihiro[1]; YAMAMOTO, M. Hiroshi[2]; NAKAMURA, Toshikazu
([1]Gakushuin Univ.; [2]Inst. Phys. Chem. Res.)

[*J. Phys. IV France* **114**, 399–400 (2004)]

^{13}C-NMR measurements have been carried out on the quasi two-dimensional organic conductor, α-(BEDT-TTF)$_2$I$_3$. We measured the angular dependence of ^{13}C-NMR spectrum at several temperatures above metal-insulator transition temperature, 135 K (= T_{MI}). We found that charge (spin) disproportionation already exists in the metallic state and gradually develops as temperature approaches to T_{MI}.

IV-C Development of Multi-Functional Molecular Systems

The molecules are usually assembled by weak intermolecular interactions and tend to retain their isolated electronic states even in the crystalline state. Consequently, the multi-functional systems can be constructed by assembling various molecules with different characters. Thus, the molecules are regarded as suitable building blocks for the bottom-up construction of the systems where various functions coexist.

Recently, "dual-action system" such as magnetic molecular conductors has attracted a considerable interest. We have discovered many molecular conducting systems exhibiting various dual-active electromagnetic properties such as the organic superconductor exhibiting a "superconductor → insulator transition" at low temperature (λ-$(BETS)_2Fe_xGa_{1-x}Cl_4$ ($0.35 < x < 0.5$) (1997)), the first antiferromagnetic organic superconductor exhibiting "antiferromagnetic superconductor → ferromagnetic metal transition" associated with meta-magnetic transition of magnetic anion layers around 1.6 T (κ-$(BETS)_2FeBr_4$ (1999–2002)), the first field-induced organic superconductor (λ-$(BETS)_2FeCl_4$ (2001)). The intriguing field-induced superconductivity was also observed in λ-$(BETS)_2Fe_xGa_{1-x}Cl_4$ and κ-$(BETS)_2FeBr_4$. Except these conductors, any hitherto-developed organic conductors scarcely show clear interplay between magnetic building blocks and conducting parts.

We have tried to prepare new TTF-type π donors with stable organic radical parts with the aim of developing new type of magnetic conductors. We are now trying to prepare new molecular conductors exhibiting spin-crossover behavior.

The large designability is another important feature of the molecular system. We have recently developed the single-component molecular metal based on the transition metal dithiolate complex with extended-TTF ligands. The fundamental idea of the molecular design of the single-component molecular metals is based on the development of multi-chalcogen π molecule with TTF-like skeleton and very small HOMO-LUMO gap. Recently the existence of the Fermi surface in the first single-component molecular metal, $[Ni(tmdt)_2]$ (tmdt = trimethylenetetrathiafulvalene) was confirmed by the observation of de Haas-van Alphen oscillation at high magnetic field.

The host-guest molecular system is a good example showing the molecular assembly by weak interactions. By utilizing weak host-guest interaction of porous materials, we are now trying to obtain new functional molecular systems.

IV-C-1 Organic Metals and Superconductors Based on BETS (BETS = Bis(ethylenedithio) tetraselenafulvalene)

KOBAYASHI, Hayao; CUI, HengBo; KOBAYASHI, Akiko[1]
([1]Univ. Tokyo)

[*Chem. Rev.* **104**, 5265 (2004)]

Since the discovery of the first organic superconductors $(TMTSF)_2X$ (TMTSF = tetramethyltetraselenafulvalene; X = PF_6, ClO_4, ...) about a quarter century ago, an extremely large progress has been achieved in the field of physics and chemistry of molecular conductors. When the metallic states of TMTSF conductors were found to be stable down to about 10 K, many chemists noticed the possibility of the existence of two-dimensional (2D) organic conductors with intermolecular 2D networks of peripheral chalcogen atoms of π molecules. In fact, by the observations of Shubnikov-de Haas (SdH) and de Haas-van Alphen (dHvA) oscillations in the subsequently developed BEDT-TTF (= bis(ethylenedithio)tetrathiafulvalene) superconductors with β- and κ-type molecular arrangements, the existence of ideally 2D organic π metal systems with stable metallic states was proved. However, in the midst of these rapid progress, an extraordinarily large impact was brought about by the discovery of high temperature cupper oxide superconductors. It became very serious for the chemists in this field to find new ways by making the best use of the merit of molecule-based systems. More than a decade ago, we started to try to prepare magnetic organic conductors based on BETS molecules and tetrahalide Fe^{3+} ions. Fortunately, the π-*d* interaction in BETS conductors was discovered to be fairly strong and we could obtain very unique magnetic organic superconductors. In this review, we have summarized our recent works on magnetic organic superconductors based on BETS and magnetic and non-magnetic anions MX_4^- (M = Fe, Ga; X = Cl, Br). Many topics such as field-induced superconductivity of λ-$(BETS)_2FeCl_4$, λ-$(BETS)_2FeBr_xCl_{4-x}$ and κ-$(BETS)_2FeBr_4$, superconductor-to-insulator transition of λ-$(BETS)_2Fe_xGa_{1-x}Cl_4$, antiferromagnetic organic superconductors, κ-$(BETS)_2FeX_4$ and switching behavior of electrical properties of magnetic organic superconductors are described.

IV-C-2 Single-Component Molecular Metals with Extended-TTF Dithiolate Ligands

KOBAYASHI, Akiko[1]; FUJIWARA, Emiko[1]; KOBAYASHI, Hayao
([1]Univ. Tokyo)

[*Chem. Rev.* **104**, 5243 (2004)]

It has been believed for a long time that the formation of electronic bands and the generation of charge carriers by the intermolecular charge transfer between the molecules constituting the band (designated by A) and other chemical species (designated by B) are two essential requirements to design molecular metals. In some cases, both molecules A and B form conduction bands where the electron and the hole carriers are generated on both A and B molecules. This is the reason why the design of metals composed of single-compo-

nent molecules is difficult. However, we have recently noticed the possibility of carrier generation even in the single-component molecular crystal and prepared the first example of the crystal of a neutral transition metal complex with extended-TTF ligands, $[Ni(tmdt)_2]$ (tmdt = trimethylenetetrathiafulvalenedithiolate) exhibiting metallic behavior down to very low temperature. More recently, a direct experimental evidence for the Fermi surface in $[Ni(tmdt)_2]$ was obtained by detecting the quantum oscillations in magnetization at very high magnetic field (or de Haas-van Alphen (dHvA) effect). Torque magnetometry measurements of single crystals of $[Ni(tmdt)_2]$ using a sensitive microcantilever at low temperature revealed dHvA oscillatory signals for all directions of magnetic field, showing the presence of three-dimensional (3D) electron and hole Fermi surfaces. Thus the existence of single-component molecular metal has been definitely confirmed.

This review describes the frontier orbital engineering for the design of single-component molecular metal and present some examples of recently developed single-component molecular conductors with various extended-TTF ligands such as $[Ni(dmdt)_2]$, $[Au(tmdt)_2]$ exhibiting magnetic transition around 85 K without loss of its high conductivity and $[Co(dt)_2]$ with unique dimeric conformation and high conductivity down to 0.6 K. Experimental evidences showing the validity of our idea on the molecular design of single-component molecular metals are also presented.

IV-C-3 Observation of Three-Dimensional Fermi Surfaces of Single-Component Molecular Metal, $Ni(tmdt)_2$

TANAKA, Hisashi[1]; TOKUMOTO, Madoka[1]; ISHIBASHI, Shouji[1]; GRAF, D.[2]; CHOI, E. S.[2]; BROOKS, J. S.[2]; YASUZUKA, Shyuma[3]; OKANO, Yoshinori; KOBAYASHI, Hayao; KOBAYASHI, Akiko[4]
([1]AIST; [2]Florida State Univ.; [3]Natl. Inst. Mater. Sci.; [4]Univ. Tokyo)

[*J. Am. Chem. Soc.* **126**, 10518 (2004)]

We have recently reported that the metal electrons can be spontaneously produced by self-assembling of the well-designed π complex molecules with TTF-like ligands and very small HOMO-LUMO gap. We have also reported that the first single-component molecular metal, $[Ni(tmdt)_2]$ and analogous compounds show the very broad low-energy electronic excitation spectra in IR region, which undoubtedly shows the validity of our molecular design of the single-component molecular metals. However, considering that there has been no example of the molecular metal composed of single molecules before our discovery, unambiguous evidence will be desired to establish completely the existence of the metal electrons in the single-component molecular crystal. One of the most rigorous evidence may be the observation of de Haas-van Alphen oscillation. Since the crystals of $[Ni(tmdt)_2]$ were very small, a new micro-cantilever technique of magnetization measurement was adopted using the hybrid magnet at the National High Magnetic Field Laboratory at Florida. The quantum oscillation observed for all the direction of the magnetic field suggested the existence of the three-dimensional Fermi surfaces.

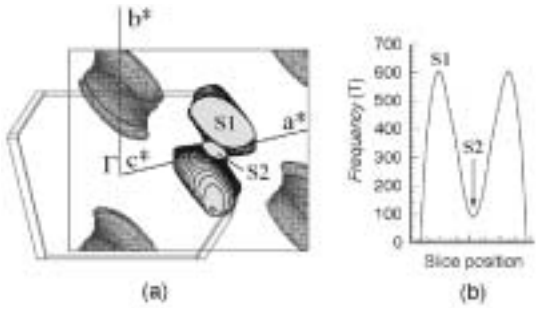

Figure 1. (a) Hole (black) and electron (gray) Fermi surfaces and the first Brillouin zone of $[Ni(tmdt)_2]$. The extremal hole orbits for the field applied parallel to c^* axis are also shown. (b) S1 and S2 are the corresponding extremal cross section sizes calculated by slicing Fermi surfaces.

IV-C-4 Syntheses, Structures and Physical Properties of New Nickel Bis(dithiolene) Complexes Containing TTF (Tetrathiafulvalene) Units

FUJIWARA, Emiko[1]; KOBAYASHI, Akiko[1]; FUJIWARA, Hideki; KOBAYASHI, Hayao
([1]Univ. Tokyo)

[*Inorg. Chem.* **43**, 1122 (2004)]

To contribute to the development of single-component molecular metals, several nickel complexes with cyclohexeno-condensed or ethylenedioxy-substituted TTF (tetrathiafulvalene) dithiolate ligands, $(R_4N)_n[Ni(chdt)_2]$ [R = Me, n = 2: (**1**); R = ^{n}Bu, n = 1: (**2**); n = 0: (**3**)] and $(R_4N)_n[Ni(eodt)_2]$ [R = Me, n = 2: (**4**); R = ^{n}Bu, n = 1: (**5**); n = 0: (**6**)], were prepared. X-Ray structures were determined on the monoanionic species (**2**) and (**5**). The tetra-*n*-butylammonium complexes of the monoanionic $[Ni(chdt)_2]$ (**2**) with a 1:1 composition revealed that its magnetic susceptibility gave good agreement with the Bonner-Fisher model (J/k_B = –28 K), which was derived from the one-dimensional chains of anions with regular intervals. On the other hand, the magnetic susceptibility of tetra-*n*-butylammonium complexes of monoanionic $[Ni(eodt)_2]$ (**5**) showed Curie-Weiss behavior (C = 0.376 K·emu·mol^{-1} and θ = –4.6 K). Both of the monoanionic species (**2**) and (**5**) indicate that they belong to the s = 1/2 magnetic systems and have relatively large and anisotropic g-values, suggesting the contribution of the nickel 3*d* orbital. The electrical resistivity measurements were performed on the compressed pellets of the neutral species (**3**) and (**6**). The fairly large conductivities were obtained (σ_{rt} = 1–10 S·cm^{-1}). In addition, in spite of the compressed powder pellet sample, the neutral species (**6**) showed metallic behavior down to *ca.* 120 K and retained high conductivity even at 0.6 K [σ(0.6 K)/$\sigma_{rt} \approx$ 1/30], suggesting the crystal to be essentially metallic down to very low temperature. These electrical behavior and Pauli paramagnetism of (**6**) indicate the system to be a new single-component metal.

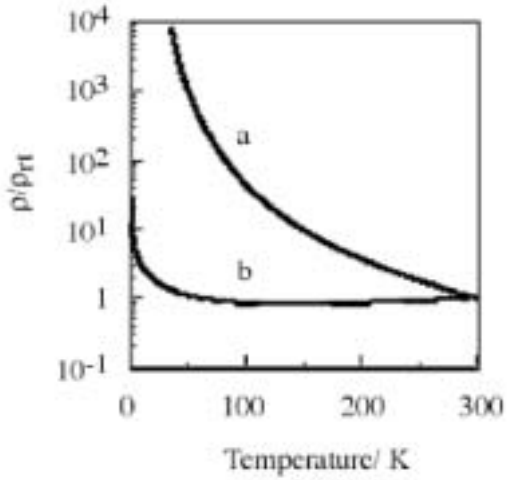

Figure 1. Temperature dependence of electrical resistivities of the neutral nickel complexes measured by use of the compressed pellets. (a)[Ni(chdt)$_2$] (**3**) and (b) [Ni(eodt)$_2$] (**6**).

IV-C-5 The Pressure Effect on the Antiferromagnetic and Superconducting Transitions of κ-(BETS)$_2$FeBr$_4$

OTSUKA, Takeo; CUI, HengBo; FUJIWARA, Hideki; KOBAYASHI, Hayao; FUJIWARA, Emiko[1]; KOBAYASHI, Akiko[1]
([1]Univ. Tokyo)

[*J. Mater. Chem.* **14**, 1682 (2004)]

Among a wide variety of highly conducting molecular solids, a special group of conducting salts, so-called π–*d* system has attracted much concern in recent years, where π–*d* system is a class of complexes comprising π conducting electrons and localized magnetic moments of transition metal ions together in a crystal. The main interests in these systems are concentrated on the possible multi-functional properties originating from the interplay between localized magnetic moments and π metal electrons because the development of the multi-functional molecular conductors is considered to be an important step for realising molecular devices. However, up to now only a very limited number of systems are known to exhibit physical properties clearly reflecting π–*d* coupling. The first antiferromagnetic organic superconductor, κ-(BETS)$_2$FeBr$_4$ shows a unique successive phase transition from paramagnetic metal to antiferromagnetic metal to antiferromagnetic superconductor with lowering temperature. In order to examine the pressure effect on the antiferromagnetic and superconducting transition (T_N, T_c), the resistivity was measured up to 6 k bar along two directions. One direction is perpendicular to the conduction plane (*I*//*b* axis), and another is parallel to the conduction plane (*I*//*a*). These resistivities along the *a* and *b* axes gave almost the same temperature dependencies though the anisotropy of the resistivity is fairly large ($\rho_{//b}/\rho_{//a} \approx 200$ at room temperature). The pressure dependencies of T_N and T_c were obtained from the anomalies in the temperature dependencies of the resistivities. The value of T_c decreased with pressure and became less than 0.5 K around 4 kbar. While, T_N was enhanced at high pressure. The high-pressure resistivity measurements under magnetic field showed the critical magnetic field of metamagnetic transition increased gradually with pressure.

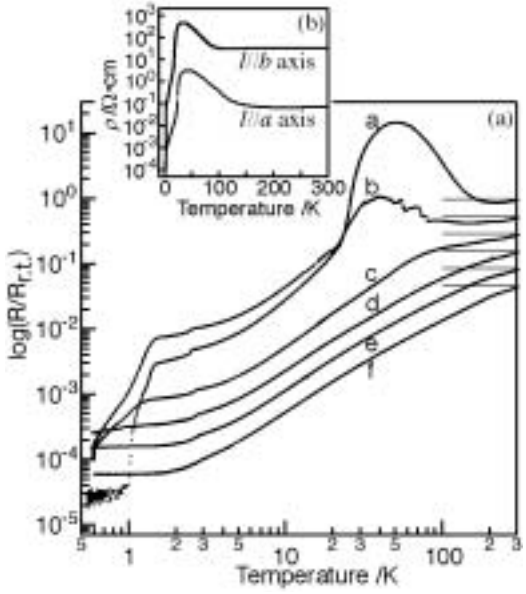

Figure 1. Temperature dependence of the resistivity of κ-(BETS)$_2$FeBr$_4$ at high pressure (< 5 kbar): a, 1 bar(ambient); b, 2 kbar; c, 3 kbar; d, 3.5 kbar; e, 4 kbar; f, 5 kbar. (b) The temperature dependencies of the resistivities of κ-(BETS)$_2$FeBr$_4$ for *I*//*a* and *I*//*b* at ambient pressure.

IV-C-6 Crystal Structure of [(C$_2$H$_5$)$_2$(CH$_3$)$_2$N][Pd(dmit)$_2$]$_2$ at High Pressure

OKANO, Yoshinori; ADACHI, Takafumi[1];NARYMBETOV, Bakhyt[2]; KOBAYASHI, Hayao; ZHOU, Biau[3]; KOBAYASHI, Akiko[3]
([1]SPring8, JASRI; [2]Uzbek Acad. Sci.; [3]Univ. Tokyo)

[*Chem. Lett.* 938 (2004)]

We have recently reported the crystal structure of high-pressure molecular superconductor, [(C$_2$H$_5$)$_2$(CH$_3$)$_2$N][Pd(dmit)$_2$]$_2$ based on the high-pressure X-ray data obtained more than several years ago. The crystal of [(C$_2$H$_5$)$_2$(CH$_3$)$_2$N][Pd(dmit)$_2$]$_2$ belongs to the triclinic system. Since the (C$_2$H$_5$)$_2$(CH$_3$)$_2$N$^+$ cation is on the inversion center, the cation is disordered with taking two possible positions randomly at ambient pressure. The Pd(dmit)$_2$ molecules are stacked face-to-face to form dimeric columns along the *a* direction. Despite of the high room-temperature conductivity, the crystal becomes semiconducting at low temperature. But as mentioned above, the system shows a superconducting transition at high pressure at 2–7 kbar. However, in contrast to most of the molecular superconductors with stable metallic states above the critical pressures where the superconducting phases are suppressed, the insulating state appears above 7 kbar. The high-pressure X-ray experiments were made by using a specially designed diamond anvil cell. The crystals with typical dimensions of about 0.3 × 0.2 × 0.04 mm^3 were used.

The X-ray diffraction spots were detected by X-ray imaging plate system equipped with a rotating anode X-ray generator (MoKα). The crystal structure determination at 10 kbar was made using the 815 reflections ($I > 3\sigma(I)$). The correction for X-ray absorption by diamond anvil was not made. Due to the limited number of the observed reflections and the relatively large number of crystallographically independent atoms (41 non-hydrogen atoms of $[(C_2H_5)_2(CH_3)_2N][Pd(dmit)_2]_2$), the anisotropic temperature factors were used only for two Pd atoms. The structure refinements gave the final *R*-value of 0.105. The band structure at high-pressure was calculated based on the high-pressure structure. The calculated orbital levels of HOMO and LUMO at ambient pressure were significantly smaller than those at 10 kbar, which is considered to be related to the increase of planarity of $Pd(dmit)_2$ molecule (or π conjugation of the molecule) at high pressure.

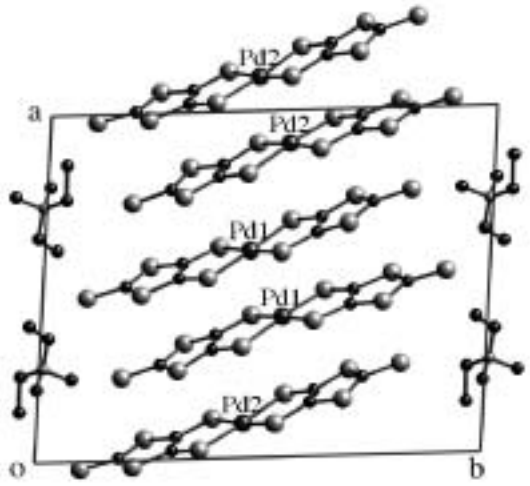

Figure 1. The crystal structure of $[(C_2H_5)_2(CH_3)_2N][Pd(dmit)_2]_2$ at 10 kbar.

IV-C-7 Synthesis, Structures and Physical Properties of a New Organic Conductor Containing a Stable PROXYL Radical

FUJIWARA, Hideki; LEE, Ha-Jin; CUI, HengBo; KOBAYASHI, Hayao; FUJIWARA, Emiko[1]; KOBAYASHI, Akiko[1]
([1]Univ. Tokyo)

[*Adv. Mater.* **16**, 1765 (2004)]

By the recent intensive studies on the molecule-based materials consisting of conducting organic layers and inorganic anion layers with localized magnetic moments, ferromagnetic metals, para- or antiferromagnetic superconductors and organic conductors exhibiting superconductor-to-insulator transition and field-induced superconductivity have been discovered. On the other hand, the development of organic ferromagnetic metals had been stimulated by the theoretical report that pointed out the possibility of the realization of ferromagnets employing the charge transfer complexes with stable organic radical substituents, and several research groups have investigated on the synthesis of donor or acceptor units bearing a stable radical part and reported cation radical salts based on such component molecules so far. However, it was quite difficult to obtain highly conducting cation radical salts because of so large steric hindrance of stable radical parts to construct the conduction pathway by stacking the conducting units such as the TTF (tetrathiafulvalene) skeleton. Recently, we have tried to overcome such problems by introducing π-extended donor skeletons which are regarded as being effective to establish sufficient intermolecular overlap integrals and π conduction bands which are indispensable for realizing the highly conducting complexes. We have discovered highly conducting cation radical salts by use of the bis-fused TTF skeleton called as TTP containing a PROXYL radical substituent and succeeded in the structure analysis of the AsF_6^- salt of cyclopentenofused TTP derivative carrying a stable PROXYL radical part having a 4:1 stoichiometry of D:A. Though the size of the crystal was very small (maximum dimension is about 0.15 mm) and the crystal quality was poor, we performed successfully a four-probe resistivity measurement. The crystal was semiconducting with the room temperature conductivity of about 1 S cm^{-1} and a small activation energy of 0.05 eV. The SQUID susceptibility measurements and ESR experiments suggested the coexistence of the localized PROXYL radical spins and π conduction electrons at high temperature ($T > 100$ K).

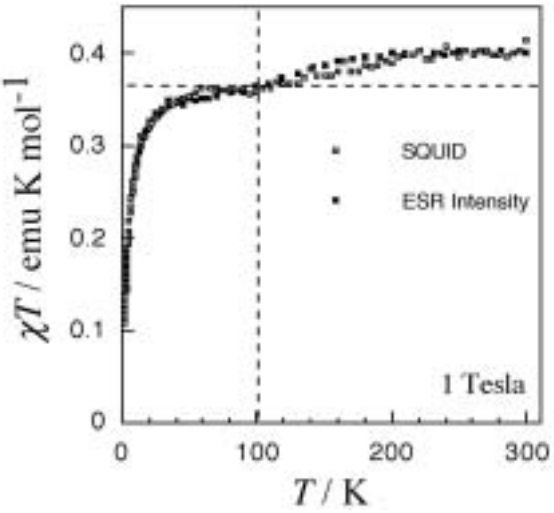

Figure 1. Temperature dependence of the χT values of $(TTP\text{-}PROXYL)_4AsF_6$ measured by SQUID (open square) and normalized ESR intensities.

IV-C-8 Anionic NaCl-Type Frameworks of $[Mn^{II}(HCOO)_3^-]$, Templated by Alkylammonium, Exhibit Weak Ferromagnetism

WANG, Zheming[1]; ZHANG, Bin[2];OTSUKA, Takeo; INOUE, Katsuya; KOBAYASHI, Hayao; KURMOO, Mohamedally[3]
([1]Peiking Univ; [2]Chinese Acad. Sci.; [3]Inst. Phys. Chim. Matériaux Strasbourg)

[*Dalton Trans.* 2209–2216 (2004)]

We present the synthesis, characterization by IR, TGA, single crystal X-ray structure and magnetic prop-

erties of a novel series of NaCl-type frameworks of $[AmineH^+][Mn(HCOO)_3^-]$, templated by alkylammonium. The anionic NaCl-framework of $[Mn(HCOO)_3^-]$ is counter-balanced by the alkylammonium cations located in the cavities of the framework to which they are hydrogen-bonded. The divalent manganese ions have octahedral geometry and are bridged by the formate in an *anti-anti* mode of coordination. All the compounds exhibit long-range antiferromagnetism below 9 K with a slight non-collinear arrangement of the moments. The canting, likely due to second-order spin-orbit coupling, is *via* a Dzyaloshinski-Moriya antisymmetric exchange mechanism. A spin-flop is observed in each case at fairly low fields. An orthorhombic to monoclinic transformation was observed for the protonated cyclotrimethyleneamine that is accompanied by localization of the cations into two positions below 240 K from the rapid dynamic flipping of the ring observed at room temperature.

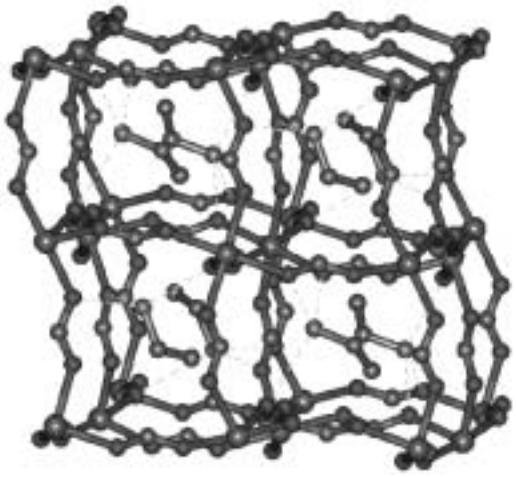

Figure 1. NaCl-type framework of $[Mn^{II}(HCOO)_3^-]$ including annmonium cations ($CH_3CH_2NH_3^+$) in the cavity.

IV-C-9 Preparation and Properties of Novel Fe(III) Spin-Crossover Complexes with $[Ni(dmit)_2]$ Anion

TAKAHASHI, Kazuyuki; KOBAYASHI, Hayao; EINAGA, Yasuaki[1]; SATO, Osamu[2]
([1]Keio Univ.; [2]KAST)

Spin-crossover phenomena are observed in transition metal complexes with d^4 to d^7 configuration under an appropriate octahedral ligand field. The spin conversion is induced by external perturbation such as temperature, pressure, light, and so on. Thus, the spin-crossover complexes are considered as a promising candidate for molecular switching materials. Recently, great attention has been attracted to development of novel multifunctional materials. We have explored possibility to control electrical conductivity by external perturbation. Since molecular-based conductors consist of relatively weak intermolecular interactions, bandwidth and band-filling can be controlled by substitution with similar size and shape of constituents. The spin conversion between the low-spin and the high-spin states accompanies a remarkable structural change in coordination bond length. Therefore, electrical conductivity is expected to be controlled by embedding of the spin-crossover ion in molecular-based conductors. We have focused our attention upon the Fe(III) spin crossover complex, $[Fe(qsal)_2]X$, and the molecular-based conducting salt, $M[Ni(dmit)_2]$ [qsalH = *N*-(8-quinolyl)-salicylaldimine, dmit = 4,5-dithiolato-1,3-dithiole-2-thione]. We have prepared and characterized novel Fe(III) spin crossover complexes with $[Ni(dmit)_2]$ anion. The syntheses of $[Fe(qsal)_2]_2[Ni(dmit)_2]$ and $[Fe(qsal)_2][Ni(dmit)_2]\cdot CH_3CN$ could be achieved by metathesis between $[Fe(qsal)_2]Cl$ and $(Bu_4N)_2[Ni(dmit)_2]$, and between $[Fe(qsal)_2]Cl$ and $(Bu_4N)[Ni(dmit)_2]$, respectively, in acetonitrile. The composition ratios of them were determined by microanalysis. Temperature dependence of $\chi_M T$ in $[Fe(qsal)_2]_2[Ni(dmit)_2]$ revealed that a gradual spin transition from the low-spin to high-spin states occurred above 150 K. However, a complete spin conversion to the high-spin state could not be observed. On the other hand, temperature dependence of $\chi_M T$ in $[Fe(qsal)_2][Ni(dmit)_2]\cdot CH_3CN$ showed a wide hysteresis with about 35 K (Figure 1). These results suggested that there was no intermolecular interaction between $[Fe(qsal)_2]$ ions in the 2:1 complex, whereas a strong cooperative interaction between them existed in the 1:1 complex. The crystal structure analyses were performed on a single crystal of both $[Fe(qsal)_2]_2[Ni(dmit)_2]$ and $[Fe(qsal)_2][Ni(dmit)_2]\cdot CH_3CN$. In $[Fe(qsal)_2]_2[Ni(dmit)_2]$, crystallographical independent molecules were one $[Fe(qsal)_2]$ ion and a half $[Ni(dmit)_2]$ ion. No interaction was observed between neither $[Fe(qsal)_2]$ nor $[Ni(dmit)_2]$ ions. On the other hand, in $[Fe(qsal)_2][Ni(dmit)_2]\cdot CH_3CN$, two-dimensional network was formed by π-π interactions between the π-ligands in $[Fe(qsal)_2]$ ion. These results were consistent to temperature dependence of magnetic behaviors. The LIESST (Light-induced excited spin state trapping) experiment and an attempt to obtain conducting complexes by electrocrystallization of $[Fe(qsal)_2][Ni(dmit)_2]\cdot CH_3CN$ are now in progress.

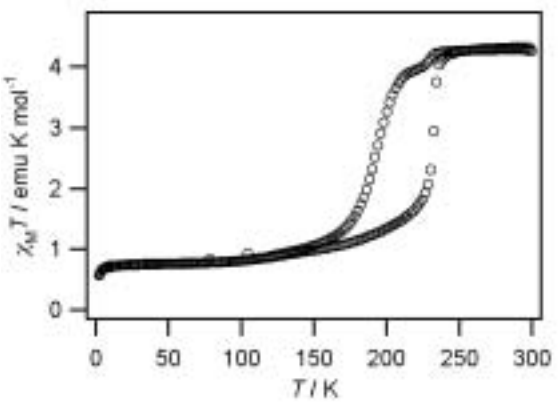

Figure 1. $\chi_M T$ *vs.* T plot of $[Fe(qsal)_2][Ni(dmit)_2]\cdot CH_3CN$. Scan speed = 2 K min^{-1}, magnetic field = 5000 G.

IV-C-10 Preparation and Characterization of Novel TTP Derivatives Connected with a Stable Organic Radical by a Long Covalent Bond Spacer

TAKAHASHI, Kazuyuki; CUI, HengBo;

FUJIWARA, Hideki[1]; KOBAYASHI, Hayao; FUJIWARA, Emiko[2]; KOBAYASHI, Akiko[2]
([1]Osaka Prefecture Univ.; [2]Univ. Tokyo)

Recently, great attention has been attracted to interplay between conducting electrons and localized spins to develop novel magneto-electronic materials. We have reported synthesis and properties of several π-donor molecules with stable organic radicals and their conducting complexes. However, since the radical part is usually bulky, we often encountered difficulties in the formation of the conduction path based on the overlap of π-donor parts. A moderate distance between the π-donor and organic radical parts is considered to decrease a hindrance to the formation of conduction path. Therefore, we have designed novel tetrathiapentalene (TTP) derivatives attached to a stable organic radical by a long covalent bond.

New TTP derivatives with stable TEMPO radicals (**3**) were synthesized by the reaction between S-protected TTPTM (**1**) and iodoalkyl-substitued TEMPO (**2**). These donors were isolated as a fine powder or film-like solid, and were unstable in air. Characterization of new donor molecules was carried out by MALDI-TOF mass spectroscopy, ESR spectra, and cyclic voltammetry. On the MALDI-TOF measurement, $[M+H]^+$ ions were observed in all new donors. ESR spectra showed triplet signals, indicating that there is a TEMPO radical in each molecule. Cyclic voltammogram of them revealed that the redox behavior of the donor part was independent of that of the TEMPO one. Preparation of the conducting complexes of these donors is now in progress.

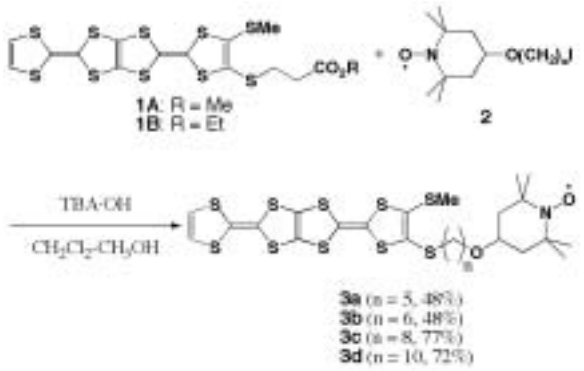

Scheme 1. Synthesis of TTP donors with a stable TEMPO radical.

IV-C-11 Crystal Structures and Physical Properties of Novel Molecular Conductors Based on BETS and MX_4^- (M = In, Tl; X = Cl, Br) Anions

CUI, HengBo; OKANO, Yoshinori; OTSUBO, Saika; TAKAHASHI, Kazuyuki; KOBAYASHI, Hayao; KOBAYASHI, Akiko[1]
([1]Univ. Tokyo)

So far we have reported many molecular conductors based on BETS and MX_4^- (M = Fe, Ga; X = Cl, Br) anions with various structure types (α, θ, κ, λ, λ'). Among them, κ-$(BETS)_2FeBr_4$ and κ-$(BETS)_2FeCl_4$ are the first and second antiferromagnetic superconductors and λ-$(BETS)_2FeCl_4$ is the first organic conductor exhibiting a field-induced superconductivity. In λ-$(BETS)_2FeCl_4$, BETS molecules are stacked to form a tetradic column along the *a* axis. There exist many shortest distance between S(Se)···Cl and therefore the strong π-*d* interaction through Cl 3*p* orbitals is expected in λ-$(BETS)_2FeCl_4$. λ'-$(BETS)_2GaBr_4$ also has triclinic lattice and tetradic columns. But unlike superconducting λ-$(BETS)_2GaCl_4$, this salt seems to have a non-magnetic insulating ground state. Recently, we have found the salts with another modified λ-type structure, λ"-$(BETS)_2TlBr_4$. Similar to the λ-type structure, λ"-type has a triclinic unit cell. BETS molecules are staked to form 8-fold column, and tetrahedral $TlBr_4^-$ anions are arranged to take the orientation of "up–up–down–down" along the 8-fold BETS column. The crystal has a fairly high conductivity but slightly semiconducting. $(BETS)_3InCl_5(PhCl)_{0.5}$ has a unique three-dimensional donor arrangement, and retains its metallic state down to 120 K with high room-temperature conductivity (250 Scm^{-1}). Two-dimensional Fermi surface was obtained by tight-binding band calculation.

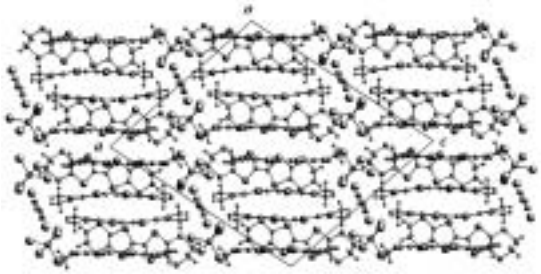

Figure 1. Crystal structure of $(BETS)_3InCl_5(PhCl)_{0.5}$.

IV-C-12 Structural and Physical Properties of Molecular Conductors Based on BEST and MX_4^- (M = Fe, Ga, In; X = Cl, Br)

CUI, HengBo; OTSUBO, Saika; OKANO, Yoshinori; TAKAHASHI, Kazuyuki; KOBAYASHI, Hayao; KOBAYASHI, Akiko[1]
([1]Univ. Tokyo)

We have reported novel λ and κ-type salts based on BETS (bis(ethylenedithio)tetraselenafulvalene) and MX_4^- (M = Fe; X = Cl, Br). These salts exhibit many unprecedented electro-magnetic properties originated from the interplay between π conduction electrons and localized 3*d* magnetic moments. Recently, we have prepared BEST (bis(ethylenediseleno)tetrathia fulvalene), and grew the crystals of molecular conductors using MX_4^- (M = Fe, Ga, In; X = Cl, Br) anions. We obtained λ-$BEST_2MCl_4$ (M = Fe, Ga) and another triclinic modification, $BEST_2MBr_4$ (M = Fe, In). λ-$BEST_2MCl_4$ (M = Fe, Ga) is isostructural to λ-$BEST_2MCl_4$ (M = Fe, Ga) but is semiconducting. In the crystal of $BEST_2MBr_4$ (M = Fe, In), BEST molecules form two kind of diadic columns along *b* axis. There exist many short S(Se)···Br contacts between BEST molecules and $FeBr_4^-$. Thus, it seems possible that intermolecular interaction through the intermolecular overlapping between π orbitals of BEST and d-like orbitals of the

anion. The resistivity of $BEST_2FeBr_4$ takes minimum around 180 K (Fe salt).

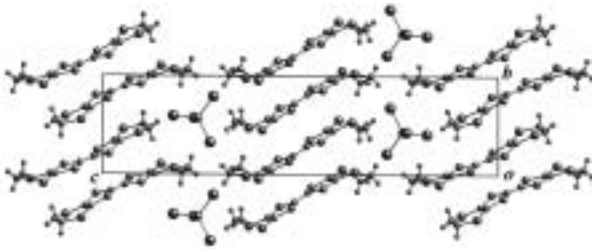

Figure 1. The crystal structure of $BEST_2FeBr_4$.

IV-C-13 Unsymmetrical Donors Fused with Pyridazine and Pyrazine Rings

OTSUBO, Saika; TAKAHASHI, Kazuyuki; CUI, HengBo; KOBAYASHI, Hayao; FUJIWARA, Hideki[1]; FUJIWARA, Emiko[2]; KOBAYASHI, Akiko[2]

([1]Osaka Prefecture Univ.; [2]Univ. Tokyo)

We have reported the crystal structures and physical properties of a series of organic conductors consisting of Se-containing π donors, bis(ethylenedithio)tetraselenafulvalene (BETS) and metal tetrahalide monoanions such as κ -and λ-$(BETS)_2MX_4$ (M = Ga, Fe, In, Tl,…; X = Br, Cl). In order to enhance the interaction between donor and anion layers, we have synthesized unsymmetrical donors fused with a pyridazine ring and a pyrazine ring **2**–**4** and prepared several cation radical salts of **3** and PEDTTSeF (**2**) by electrochemical oxidation. The ReO_4^- salt of **3** has 1:1 donor-to-anion composition, which exhibited a semiconducting behavior (σ_{rt} = 0.45 S/cm, E_a = 0.094 eV). Whereas $(PEDTTSeF)_2FeX_4$ (X = Br, Cl) showed a metallic behavior down to 60 K (X = Cl) or 120 K (X = Br). The temperature dependence of magnetic susceptibility suggested very weak magnetic interactions between donors and anions.

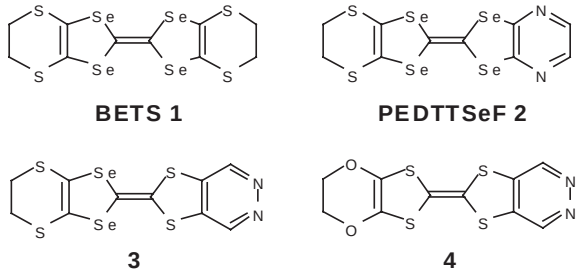

Figure 1. Molecular structures of organic donors.

IV-C-14 A Novel TTP Donor Containing a Stable Organic Radical

OTSUBO, Saika; TAKAHASHI, Kazuyuki; CUI, HengBo; LEE, Ha-Jin; KOBAYASHI, Hayao; FUJIWARA, Hideki[1]; FUJIWARA, Emiko[2]; KOBAYASHI, Akiko[2]

([1]Osaka Prefecture Univ.; [2]Univ. Tokyo)

Development of magnetic conductors bearing both conductivity and magnetism has recently played a important role in the research of the multifunctionality of organic molecular materials. Recently, we have synthesized several organic donors containing a TEMPO (2,2,6,6-tetramethylpiperidin-1-yloxyl) radical or a PROXYL (2,2,5,5-tetramethylpyrrolidin-1-yloxyl) radical. Among them, TTPPROXYL was found to produce interesting conductors exhibiting the coexistence of the conduction electrons and the localized spins. However, TTPPROXYL gives racemic compounds. So, a new TTP donor containing 2,2,5,5-tetramethyl-3-pyrrolin-1-yloxyl was synthesized as orange powder in 0.43% yield (14 steps from 2,2,6,6-tetramethyl-4-piperidinone). The preparation of cation radical salts by electrochemical oxidation is now in progress.

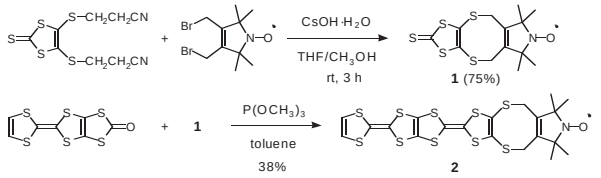

Scheme 1. Synthetic route of a new organic donor.

IV-C-15 Organic Conductors Containing a TEMPO Radical

OTSUBO, Saika; TAKAHASHI, Kazuyuki; CUI, HengBo; KOBAYASHI, Hayao; FUJIWARA, Hideki[1]; FUJIWARA, Emiko[2]; KOBAYASHI, Akiko[2]

([1]Osaka Prefecture Univ.; [2]Univ. Tokyo)

We have reported many intriguing electro-magnetic properties discovered in the magnetic organic superconductors based on Se-containing π donors BETS and magnetic transition metal anions FeX_4^- (X = Cl, Br). Besides BETS conductors, an attempt to obtain new type of magnetic organic conductors has been also performed by using donors containing a TEMPO (2,2,6,6-tetramethylpiperidin-1-yloxyl) radical or NN (4,4,5,5-tetramethyl-2-imidazoline-1-oxyl-3-oxide). TEMPOET (**2**), which is constituted of ET part and TEMPO radical part, has been synthesized several years ago but no highly conducting salts has not been prepared yet. We have recently tried to prepare similar TEMPOET-type organic donors (**1**, **3**–**5**), which were synthesized by cross-coupling reaction and Horner-Wittig reaction (10–20% yield, 2 steps). Several cation radical salts with tetrahedral anions ($FeCl_4^-$, BF_4^-,…) were prepared by electrochemical oxidation. However, up to now, highly conducting salt could not be obtained.

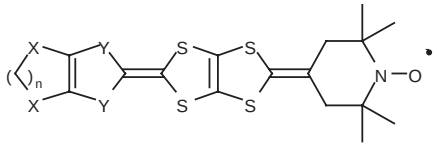

1 (n = 1, X = Y = S)
2 (n = 1, X = Y = S) [**TEMPOET**]
3 (n = 3, X = Y = S)
4 (n = 2, X = S, Y = Se)
5 (n = 2, X = Se, Y = S)

Figure 1. Organic donors with TEMPO radical parts.

IV-D Electronic and Magnetic Properties of π-Electron-Based Molecular Systems

π-electrons are an interesting building block in architecting functionalized electronic and magnetic molecular systems. We have focused on nano-sized graphite and TTF-based organic charge transfer complexes, in which π-electrons play an important role, in developing new types of molecular electronic systems. In nanographene, single layer nanographite, which is defined as flat open π-electron system have edges and contrasted to closed π-electron systems of fullerenes and carbon nanotubes, non-bonding π-electronic state appearing around the Fermi level generates unconventional nanomagnetism. We have found an interesting electronic wave interference effect in finite-sized graphite with distortion-network structures and anisotropy of the Raman spectra of nanographite ribbons. A combination of TTF-based π-electron donor and counteranion having localized spins is a useful way in producing molecular magnetic conductors, which are expected to have properties different from traditional metal magnets featured with *s-d* interaction. Under this scheme, we have developed a new class of TTF-based organic magnetic conductors. The interaction between the conducting π-electrons of donors and the localized *d*-electrons of magnetic anions are found to show interesting interplay between magnetism and electron transport.

IV-D-1 Weak-Ferromagnetism in Molecular Magnets Based on Transition Metal Complexes of Crown Thioether

NISHIJO, Junichi[1]; NIYAZAKI, Akira[1]; ENOKI, Toshiaki[2]
([1]Tokyo Inst. Tech.; [2]IMS and Tokyo Inst. Tech.)

[*Polyhedron* **22**, 1755–1758 (2003)]

A new class of molecular based magnets $M(9S3)_2[Ni(bdt)_2]_2$ (M = Ni, Co) consisting of transition metal complex of crown thioether show weak-ferromagnetic transitions at T_N = 6.2 and 2.6 K for M = Ni and Co, respectively, accompanied by remanent magnetizations $0.2\mu_B$ and $0.01\mu_B$ with coercive forces 200 and 10 Oe. $M(9S3)_2^{2+}$ cations (S = 1 and 1/2 for M = Ni and Co, respectively), and a half of $Ni(bdt)_2^-$ (S = 1/2) anions form alternate antiferromagnetic (AF) chains (#1), while the other half of $Ni(bdt)_2^-$ anions form uniform AF chains (#2). These two type of chains are connected to each other by two weak AF interactions; interaction between $Ni(bdt)_2^-$ in #1 and $Ni(bdt)_2^-$ in #2, and interaction between $M(9S3)_2^{2+}$ in #1 and $Ni(bdt)_2^-$ in the adjacent chain #1. A competition between these two AF interactions causes canted spin configuration, giving rise to weak-ferromagnetism.

IV-D-2 New Bulk Weak Ferromagnet in Ferrimagnetic Chains of Molecular Material Based on DTDH-TTP and Paramagnetic Thiocyanato Complex Anion: (DTDH-TTP)[Cr(isoq)$_2$(NCS)$_4$]

SETIFI, Fatima[1]; OUAHAB, Lahcène[1]; GOLHEN, Stéphane[1]; MIYAZAKI, Akira[2]; ENOKI, Toshiaki[3]; YAMADA, Jun-ichi[4]
([1]CNRS; [2]Tokyo Inst. Tech.; [3]IMS and Tokyo Inst. Tech.; [4]Univ. Hyogo)

[*C. R. Chim.* **6**, 309–316 (2003)]

The preparation, X-ray crystal structure and magnetic properties of a new charge transfer salt, (DTDH–TTP)$Cr(isoq)_2(NCS)_4$, DTDH–TTP = 2-(1',3'-dithiol-2'-ylidene)-5-(1",3"-dithiolan-2"-ylidene)-1,3,4,6-tetrathiapentalene, ISOQ = isoquinoline) are reported. Crystal data: monoclinic, space group *C*2/*c* (#15), a = 16.0836(5), b = 19.2488(6), c = 12.6829(6) Å, β = 95.669(1), V = 3906.5(2) Å^3, Z = 4, R = 0.0515 for 2899 reflections with $I > 2\sigma(I)$. The crystal structure consists of mixed organic and inorganic layers in the *ac*-plane, each layer being formed by mixed columns of DTDH–$TTP^{\bullet+}$ radical cations and paramagnetic metal complex anions. Short intermolecular atomic contacts between donor and anion are observed in the column in the *c* direction. Ferrimagnetic interactions are observed between the non-equivalent donor and anion spins. This material exhibits bulk canted weak ferromagnetism below T_C = 8.7 K.

IV-D-3 Anomalous Metallic State of One-Dimensional Molecular Conductor (EDO-TTFBr$_2$)$_3$I$_3$

MIYAZAKI, Akira[1]; KATO, Takehiko[1]; YAMAZAKI, Hisashi[1]; ENOKI, Toshiaki[2]; OGURA, Eiji[3]; KUWATANI, Yoshiyuki[3]; IYODA, Masahiko[3]; YAMAURA, Jun-ichi[4]
([1]Tokyo Inst. Tech.; [2]IMS and Tokyo Inst. Tech.; [3]Tokyo Metr. Univ.; [4]Univ. Tokyo)

[*Phys. Rev. B* **68**, 085108 (6 pages) (2003)]

The structure and physical properties of the one-dimensional (1D) molecular conductor (EDO-TTF$Br_2)_3I_3$ are reported. This salt is composed of quasi-1D uniform stacks of the donor molecules and counter anions which are translationally disordered at room temperature. The temperature dependence of the lattice constants shows that, as the temperature decreases, the thermal contraction takes place along the donor columns, leading to the enhancement of the one-dimensionality of the π-electron system. The electrical conductivity and thermoelectric power show a metallic conductivity down to circa 140 K, where a metal-insulator transition takes place. The transition temperature decreases to circa 60 K as the hydrostatic pressure is applied up to 1.1 GPa. Although the transport properties give the itinerant feature of the pelectrons, the static

susceptibility behaves as a 1D Heisenberg antiferromagnet-like behavior of localized spins from room temperature down to 15 K, which is consistent with the ESR linewidth governed by the 1D diffusion mechanism of localized spins. The coexistence of the itinerant character of the transport properties and the localized character of the magnetic properties of the π-electron system is attributed to the strongly correlated nature of the quasi-1D electron system.

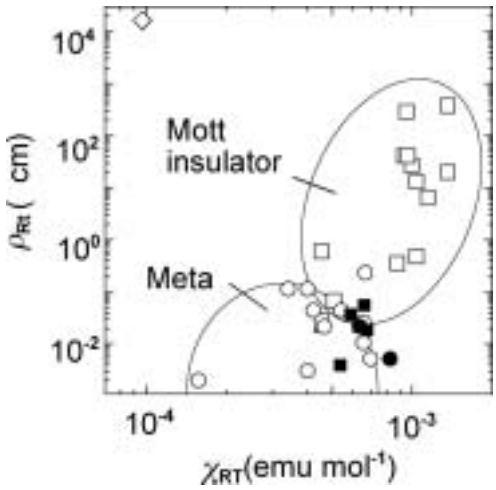

Figure 1. The diagram of the resistivities *vs.* susceptibilities at room temperature for various TTF-based salts. Filled circle: $(EDO\text{-}TTFBr_2)_3I_3$; filled squares: $(TMTTF)_2X$; squares: Mott insulators; open circles: metallic compounds; diamond: band insulator.

IV-D-4 Property of Self-Assembled Monolayers of Long-Alkyl-Chain-Substituted TTF Derivative

YOKOTA, Yasuyuki[1]; YUGE, Ryota[1]; MIYAZAKI, Akira[1]; ENOKI, Toshiaki[2]; HARA, Masahiko[3]
([1]Tokyo Inst. Tech.; [2]IMS and Tokyo Inst. Tech.; [3]RIKEN)

[*Mol. Cryst. Liq. Cryst.* **407**, 121/[517]–127/[523] (2003)]

Self-assembled monolayers (SAMs) of an electron donor TTF derivative with long alkyl chains ($-C_{11}H_{22}-$) are formed on Au(111). STM, surface plasmon resonance, and FTIR reflection absorption spectroscopy measurements suggest that TTF backbone is isolated from the gold substrate by long alkyl chains. Cyclic voltammograms reveal two redox peaks ($E_1^{1/2}$ = 263 mV, $E_2^{1/2}$ = 508 mV *vs.* Ag/Ag^+) corresponding to TTF/TTF^+ and TTF^+/TTF^{2+}. These peak currents are proportional to the scan rates, indicating that the TTF backbone maintains its electrochemical activity in the SAMs. In addition, the peak-to-peak separations between oxidation and reduction are roughly proportional to the scan rates, which indicates that a potential drop takes place at the long alkyl chains, which work as resistance in the electron transport.

IV-D-5 Magnetic Anisotropy of Cerium Endhedral Metallofullerene

INAKUMA, Masayasu[1]; TANIHARA, Atsushi[2]; KATO, Haruhito[2]; SHINOHARA, Hisanori[2]; ENOKI, Toshiaki[3]
([1]Tokyo Inst. Tech.; [2]Nagoya Univ.; [3]IMS and Tokyo Inst. Tech.)

[*J. Phys. Chem. B* **107**, 6965–6973 (2003)]

Cerium endohedral metallofullerene ($Ce@C_{82}$) is a π-*f* composite nanomagnet, where anisotropic *f*-electron spin is expected to couple with the rotational motion of the fullerene cage that has π-electron spin. The field cooling effect on the susceptibility of $Ce@C_{82}$ in organic solutions suggests that the application of a magnetic field forces the molecular orientations to be aligned, in cooperation with the magnetic anisotropy of the *f*-electron spin coupled with the molecular orientation. The role of crystal field in the magnetic anisotropy, which is associated with the off-center geometry of the Ce ion in the cage, is clarified by the crystal field analysis. The crystal field effect in the metallofullerene cage is considerably reduced, in contrast to that of ordinary rare-earth compounds. This is consistent with the findings of a small electronic coupling between the *f* and π-electrons and a shallow potential of the surrounding cage to the Ce ion. As a consequence, the crystal field effect is emphasized in the low-temperature range (below ~ 100 K).

IV-D-6 Resonance Raman Scattering in Carbon Nanotubes and Nanographites

PIMENTA, M. A.[1]; JORIO, A.[1]; DANTAS, M. S.[1]; FANTINI, C.[1]; DE SOUZA, M.[1]; CANÇADO, L. G.[1]; SAMSONIDZE, Ge. G.[2]; DRESSELHAUS, G.[2]; DRESSELHAUS, M. S.[2]; GRÜNEIS, A.[3]; SAITO, Riichiro[3]; SOUZA FILHO, A. G.[4]; KOBAYASHI, Yousuke[5]; TAKAI, Kazuyuki[5]; FUKUI, Ken-ichi[5]; ENOKI, Toshiaki[6]
([1]Univ. Federal Minas Gerais; [2]MIT; [3]Tohoku Univ., CREST JST; [4]Univ. Federal Ceará; [5]Tokyo Inst. Tech.; [6]IMS and Tokyo Inst. Tech.)

[*Molecular Nanostructures: Proceedings XVII International Winterschool on Electronic Properties of Novel Materials*, H. Kuzmany, J. Fink, M. Mehring and S. Roth, Eds., AIP Conference Proceeding **685**, page 219–224 (2003)]

In this work, we discuss the resonant Raman process in nanographites and carbon nanotubes, relating the most important Raman features to a first-order (single resonance) or a second-order (double resonance) process. We also show that, in the case of 1D systems, the term "resonance" has a more strict meaning and occurs when the energy of the photon does not simply coincide with the energy of a possible electron-hole pair, but rather matches the separation between van Hove singularities in the valence and conduction bands.

IV-D-7 Interface Effect on the Electronic Structure of Alkanethiol-Coated Platimum Nanoparticles

TU, Weixia[1]; TAKAI, Kazuyuki[1]; FUKUI, Ken-ichi[1]; MIYAZAKI, Akira[1]; ENOKI, Toshiaki[2]
([1]Tokyo Inst. Tech.; [2]IMS and Tokyo Inst. Tech.)

[*J. Phys. Chem. B* **107**, 10134–10140 (2003)]

The structure and electronic properties are investigated for Pt nanoparticles coated with octadecanethiol self-assembled monolayer. The increase in the octa decanethiol/Pt ratio from 0 to full coverage reduces the average particle size from 2.2 to 0.9 nm. The temperature-independent spin susceptibility rises upon the increase in the particle size, quantum size effect being suggested to govern the magnetism. The low-temperature susceptibility shows a large Curie-type divergence, which cannot be explained simply by the even electron state of Pt. XPS spectra suggest an electron deficiency in the interior Pt nanoparticles, which is brought about by charge transfer from nanoparticle to coating thiol monolayer. The ESR line width and the *g*-value deviation increase as the octadecanethiol/Pt ratio is elevated, which are associated with the enhancement of spin-orbit interaction at the interface between the interior nanoparticle and coating thiol monolayer. This change at the interface works to make first spin-lattice relaxation centers in the carrier scattering process.

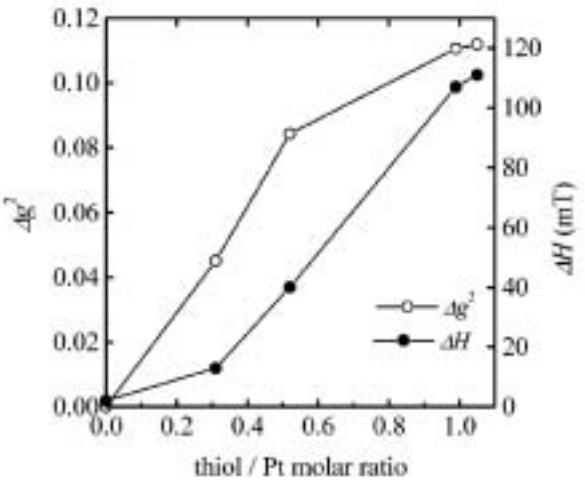

Figure 1. The thiol/Pt ratio dependence of Δg^2 and ΔH measured at room temperature for the thiol-coated Pt nanoparticles. The data for the naked Pt particle (thiol/Pt) 0) is obtained from ref 15.

IV-D-8 Tuning Magnetism and Novel Electronic Wave Interference Patterns in Nanographite Materials

HARIGAYA, Kikuo[1]; KOBAYASHI, Yousuke[2]; KAWATSU, Naoki[2]; TAKAI, Kazuyuki[2]; SATO, Hirohiko[3]; RAVIER, Jérôme[2]; ENOKI, Toshiaki[4]; ENDO, Morinobu[5]
([1]Synthetic Nano-Function Mater. Project, AIST; [2]Tokyo Inst. Tech.; [3]Chuo Univ.; [4]IMS and Tokyo Inst. Tech.; [5]Shinshu Univ.)

[*Physica E* **22**, 708–711 (2004)]

Antiferromagnetism in stacked nanographite is investigated with using the Hubbard-type models. The A–B stacking or the stacking near to that of A–B type is favorable for the hexagonal nanographite with zigzag edges, in order that magnetism appears. We also find that the open shell electronic structure can be an origin of the decreasing magnetic moment with the decrease of the inter-graphene distance, as experiments on adsorption of molecules suggest. Next, superperiodic patterns with a long distance in a nanographene sheet observed by STM are discussed in terms of the interference of electronic wave functions. The period and the amplitude of the oscillations decrease spatially in one direction. We explain the superperiodic patterns with a static linear potential theoretically. In the $k \cdot p$ model, the oscillation period decreases, and agrees with experiments. The spatial difference of the static potential is estimated as 1 :3 eV for 200 nm in distance, and this value seems to be reasonable in order that the potential difference remains against perturbations, for example, by phonon fluctuations and impurity scatterings. It turns out that the long-distance oscillations come from the electronic structure of the two-dimensional graphene sheet.

IV-D-9 Magnetic Phase Diagram of Three-Dimensional Diluted Ising Antiferromagnet $Ni_{0.8}Mg_{0.2}(OH)_2$

SUZUKI, Masatsugu[1]; SUZUKI, Itsuko[1]; ONYANGO, Tedamann M.[1]; ENOKI, Toshiaki[2]
([1]State Univ. New York Binghamton; [2]IMS and Tokyo Inst. Tech.)

[*J. Phys. Soc. Jpn.* **73**, 206–215 (2004)]

H-T diagram of 3D diluted Ising antiferromagnet $Ni_cMg_{1-c}(OH)_2$ with $c = 0.8$ has been determined from measurements of SQUID DC magnetization and AC magnetic susceptibility. At $H = 0$, this compound undergoes two magnetic phase transitions: an antiferromagnetic (AF) transition at the Néel temperature T_N (= 20.7 K) and a reentrant spin glass (RSG) transition at T_{RSG} (≈ 6 K). The *H-T* diagram consists of the RSG, spin glass (SG), and AF phases. These phases meet a multicritical point P_m (H_m = 42 kOe, T_m = 5.6 K). The irreversibility of susceptibility defined by δ (= $\chi_{FC} - \chi_{ZFC}$) shows a negative local minimum for $10 \le H \le 35$ kOe, suggesting the existence of possible glassy phase in the AF phase. A broad peak in δ and χ" at $H \ge 20$ kOe for T_N (c = 0.8, H) ≤ $T \le T_N$ (c = 1, H = 0) (= 26.4 K) suggests the existence of the Griffiths phase.

IV-D-10 STM Observation of Electronic Wave Interference Effect in Finite-Sized Graphite with Distortion-Network Structures

KOBAYASHI, Yousuke[1]; TAKAI, Kazuyuki[1]; FUKUI, Ken-ichi[1]; ENOKI, Toshiaki[2]; HARIGAYA, Kikuo[3]; KABURAGI, Yutaka[4]; HISHIYAMA, Yoshihiro[4]
([1]Tokyo Inst. Tech.; [2]IMS and Tokyo Inst. Tech.; [3]Synthetic Nano-Function Mater. Project, AIST;

[4]Musashi Inst. Tech.)

[*Phys. Rev. B* **69**, 035418 (7 pages) (2004)]

Superperiodic patterns near a step edge were observed by scanning tunneling microscopy on several-layer-thick graphite sheets on a highly oriented pyrolitic graphite substrate, where a dislocation network is generated at the interface between the graphite overlayer and the substrate. Triangular- and rhombic-shaped periodic patterns whose periodicities are around 100 nm were observed on the upper terrace near the step edge. In contrast, only outlines of the patterns similar to those on the upper terrace were observed on the lower terrace. On the upper terrace, their geometrical patterns gradually disappeared and became similar to those on the lower terrace without any changes of their periodicity in increasing a bias voltage. By assuming a periodic scattering potential at the interface due to dislocations, the varying corrugation amplitudes of the patterns can be under-stood as changes in the local density of states as a result of the beat of perturbed and unperturbed waves, *i.e.*, the interference in an overlayer. The observed changes in the image depending on an overlayer height and a bias voltage can be explained by the electronic wave interference in the ultrathin overlayer distorted under the influence of dislocation-network structures.

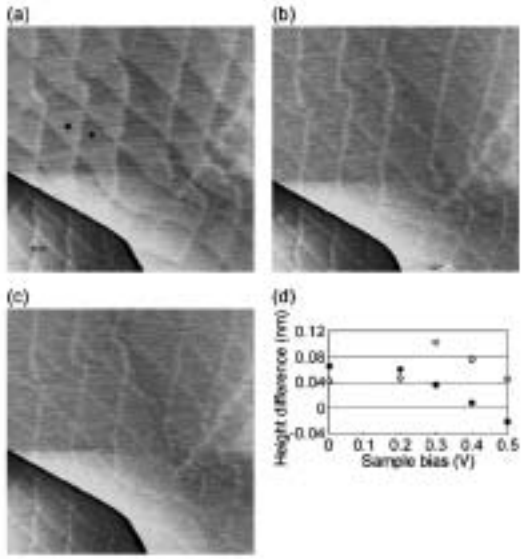

Figure 1. STM images (500 × 500 nm^2) of superperiodic patterns at higher sample bias voltages; (a) V_s = 0.3 V, (b) V_s = 0.4 V, and (c) V_s = 0.5 V. By increasing the bias voltage, the corrugation am-plitude of superperiodic patterns on the upper terrace decreased gradually [(a) and (b)] and changed into a net pattern (c). In con-trast, no significant change was observed for the pattern on the lower terrace. The net pattern appearing on the upper terrace of (c) is similar to that on the lower terrace. Height differences between two points depicted in (a) are shown in (d) for clarifying the bias-dependent contrast. Solid and blank circles are the height differ-ences of the upper and lower terrace, respectively. (Circles at the sample bias of around 0 V are the height differences at V_s = 0.02 V.)

IV-D-11 STM Observation of the Quantum Interference Effect in Finite-Sized Graphite

KOBAYASHI, Yousuke[1]; TAKAI, Kazuki[1]; FUKUI, Ken-ichi[1]; ENOKI, Toshiaki[2]; HARIGAYA, Kikuo[3]; KABURAGI, Yutaka[4];HISHIYAMA, Yukihiro[4]
([1]Tokyo Inst. Tech.; [2]IMS and Tokyo Inst. Tech.; [3]Synthetic Nano-Function Mater. Project, AIST; [4]Musashi Inst. Tech.)

[*J. Phys. Chem. Solids* **65**, 199–203 (2004)]

Superperiodic patterns were observed by STM on two kinds of finite-sized graphene sheets. One is nanographene sheets inclined from a highly oriented pyrolitic graphite (HOPG) substrate and the other is a several-layer-thick graphene sheets with dislocation-network structures against a HOPG substrate. As for the former, the in-plane periodicity increased gradually in the direction of inclination, and it is easily changed by attachment of a nanographite flake on the nanographene sheets. The oscillation pattern can be explained by the interference of electron waves confined in the inclined nanographene sheets. As for the latter, patterns and their corrugation amplitudes depended on the bias voltage and on the terrace height from the HOPG substrate. The interference effect by the perturbed and unperturbed waves in the overlayer is responsible for the patterns whose local density of states varies in space.

IV-D-12 Theoretical Study on Novel Electronic Properties in Nanographite Materials

HARIGAYA, Kikuo[1]; YAMASHIRO, Atsushi[2]; SHIOMI, Yukihiko[1]; WAKABAYASHI, Katsunoi[3]; KOBAYASHI, Yousuke[4]; KAWATSU, Naoki[4]; SATO, Hirohiko[5]; RAVIER, Jérôme[4]; ENOKI, Toshiaki[6]; ENDO, Morinobu[7]
([1]Synthetic Nano-Function Mater. Project, AIST; [2]AIST; [3]Hiroshima Univ.; [4]Tokyo Inst. Tech.; [5]Chuo Univ.; [6]IMS and Tokyo Inst. Tech.; [7]Shinshu Univ.)

[*J. Phys. Chem. Solids* **65**, 123–126 (2004)]

Antiferromagnetism in stacked nanographite is investigated with using the Hubbard-type model. We find that the open shell electronic structure can be an origin of the decreasing magnetic moment with the decrease of the inter-layer distance, as experiments on adsorption of molecules suggest. Next, possible charge-separated states are considered using the extended Hubbard model with nearest-neighbor repulsive interactions. The charge-polarized state could appear, when a static electric field is present in the graphene plane for example. Finally, superperiodic patterns with a long distance in a nanographene sheet observed by STM are discussed in terms of the interference of electronic wave functions with a static linear potential theoretically. In the analysis by the $k \cdot p$ model, the oscillation period decreases spatially in agreement with experiments.

IV-D-13 Structure and Physical Properties of Molecular Magnets Based on Trasition Metal Complexes of Crown Thioether

NISHIJO, Junichi[1]; MIYAZAKI, Akira[1]; ENOKI, Toshiaki[2]
([1]Tokyo Inst. Tech.; [2]IMS and Tokyo Inst. Tech.)

[*Bull. Chem. Soc. Jpn.* **77**, 715–727 (2004)]

A new series of molecule-based magnets, including crown thioether (9S3 = 1,4,7-trithiacyclononane) complexes of transition metals (Ni, Co, Cu), are presented. TCNQ salts $[M(9S3)_2](TCNQ)_2$ (M = Ni, Co) are one-dimensional (1D), antiferromagnetic (AF) complexes with an intra-chain interaction J = –3.9 K and –1.3 K for M = Ni and Co, respectively, despite its long inter-molecular distance, for which the large spin density on the sulfur atom in the magnetic $[M(9S3)_2]^{2+}$ cation is responsible. The mixed valence salt $[M(9S3)_2](TCNQ)_3$ (M = Ni, Co) is a paramagnetic semiconductor. 1D AF magnet $[Cu(9S3)Br_2]$ does not undergo any magnetic transition because of the weak inter-chain interaction. Substituting a very small amount (~ 5%) of Cu with Ni causes a structural change. The change decreases the distances of inter-chain S–S contacts, resulting in the generation of an AF transition at T_N = 4.5 K. $[M(9S3)_2][Ni(bdt)_2]_2$ (M = Ni, Co; bdt = 1,2-benzenedithiolato) are weak-ferromagnets with T_N = 6.2 K and 2.6 K for M = Ni and Co, respectively. In the crystals, $[M(9S3)_2]^{2+}$–$[Ni(bdt)_2]^-$ alternate chains and $[Ni(bdt)_2]^-$ uniform chains coexist. The appearance of weak-ferromagnetism is associated with a competition between two kinds of inter-chain AF interactions between $[M(9S3)_2]^{2+}$–$[Ni(bdt)_2]^-$ alternate chains, where the stronger one is an indirect inter-chain interaction through $[Ni(bdt)_2]^-$ uniform chains, while the weaker is a direct inter-chain interaction.

IV-D-14 Effect of Heat-Treatment on Magnetic Properties of Non-Graphitic Disordered Carbon

TAKAI, Kazuyuki[1]; OGA, Meigo[1]; ENOKI, Toshiaki[2]; TAOMOTO, Akira[3]
([1]Tokyo Inst. Tech.; [2]IMS and Tokyo Inst. Tech.; [3]Matsushita Electric Industrial Co., Ltd.)

[*Diamnod Rel. Mater.* **13**, 1469–1473 (2004)]

Heat-treatment effect on the electronic properties is investigated by magnetic susceptibility and ESR measurements in elation to structural change for non-graphitic but sp-rich disordered carbon thin-film prepared by pulsed laser deposition. X-ray 2 diffraction reveals that the sp y sp -jumbling “non-graphitic” structure of non-heat-treated sample with atomic-scale disorder is 23 easily relaxed into the nano-sized “graphitic” island-network by heat-treatment at approximately 600 ºC, preserving the sp^2/sp^3 ratio in the sample at ;90%. According to the temperature dependence of magnetic susceptibility, non-heat-treated sample shows the Curie-Weiss behavior with the large Pauli paramagnetic temperature-independent term and antiferromagnetic interaction whose strength is significantly larger than that simply expected from the average spin –spin distance. The temperature dependence of ESR signal intensity confirms the large contribution of the Pauli paramagnetism in the non-heat-treated sample.

IV-D-15 Development of TTF-Based Self-Assembled Monolayer Systems and Their Electronic Properties

ENOKI, Toshiaki[1]; YOKOTA, Yasuyuki[2]; YUGE, Ryota[2]; TU, Weixia[2]; MIYAZAKI, Akira[2]; TAKAI, Kazuyuki[2]; FUKUI, Ken-ichi[2]
([1]IMS and Tokyo Inst. Tech.; [2]Tokyo Inst. Tech.)

[*J. Phys. IV France* **114**, 667–671 (2004)]

Self-assembled monolayer (SAM) systems of alkanethiol and TTF-substituted alkanethiol molecules on Au substrate and metal nanoparticles are investigated. TTF-substituted alkanethiol molecules form charge transfer complex SAM with TCNQ molecules, where charge transfer (CT) rate becomes similar to that in bulk TTF·TCNQ crystal. TTF-substituted alkanethiol SAMs with long alkyl chains shows Coulomb-blockade-type electron transport owing to the resistance of the long alkyl chain bridge. In Pt nanoparticles with alkanethiol SAMs on their surface, CT takes place from core Pt nanoparticle to surface SAMs, producing an electron deficient state in Pt core nanoparticle. Pd nanoparticles with SAMs of mixtures of alkanethiol and TTF-substituted alkanethiol molecules take a large reduction of the Pauli paramagnetic susceptibility, which is brought about by CT.

IV-D-16 Crystal Structure and Physical Properties of $(EDO\text{-}TTFBr_2)_2FeX_4$ (X = Cl, Br)

MIYAZAKI, Akira[1]; AIMATSU, Masashi[1]; YAMAZAKI, Hisashi[1]; ENOKI, Toshiaki[2]; UGAWA, Kouhei[3]; OGURA, Eiji[3]; KUWATANI, Yoshiyuki[3]; IYODA, Masahiko[3]
([1]Tokyo Inst. Tech.; [2]IMS and Tokyo Inst. Tech.; [3]Tokyo Metropolitan Univ.)

[*J. Phys. IV France* **114**, 545–547 (2004)]

The crystal structure and physical properties of radical ion salts $(EDO\text{-}TTFBr_2)_2FeX_4$ (X = Cl, Br) composed of halogen-substituted organic donor and magnetic halide anions are investigated. The salts consist of uniformly stacked donor molecules, whose Br substituents are connected to halide ligands of anions with remarkably short intermolecular contacts. Both salts show metallic behavior above *ca.* 30 K. The $FeCl_4$ salt shows an antiferromagnetic (AF) transition at T_N = 4.2 K despite the absence of anion···anion contacts, thus the magnetic interaction between the localized spins on the anions is mediated by the π-*d* interaction through the Br···Cl contacts. For the $FeBr_4$ salt the AF transition temperature is elevated to T_N = 13.5 K, accompanied with another anomaly at T_{C2} = 8.5 K. This behavior can be qualitatively explained by a magnetic structure model where the π-*d* interaction between donor and anion is taken into account.

IV-D-17 Strong π-*d* Interaction Based on Brominated TTF-Type Donor $EDT\text{-}TTFBr_2$

NISHIJO, Junichi[1]; MIYAZAKI, Akira[1]; ENOKI,

Toshiaki[2]; WATANABE, Ryoji[2]; KUWATANI, Yoshiyuki[3]; IYODA, Masahiko[3]
([1]Tokyo Inst. Tech.; [2]IMS and Tokyo Inst. Tech.; [3]Tokyo Metropolitan Univ.)

[*J. Phys. IV France* **114**, 561–563 (2004)]

New π-*d* interacting system based on brominated TTF-type donor EDT-$TTFBr_2$ (= 4,5-dibromo-4',5'-ethylenedithiotetrathiafulvalene) was investigated. Magnetic $(EDT\text{-}TTFBr_2)_2FeBr_4$ and non-magnetic $(EDT\text{-}TTFBr_2)_2GaBr_4$ are isostructural salts, which have strong anion-donor interaction through Br–Br atomic contacts with weak direct anion-anion interaction. The iron salt takes an antiferromagnetic transition at T_N = 11 K owing to strong π-*d* interaction, which originates from the strong anion-donor interaction. The strong π-*d* interaction also plays an important role in the electron transport phenomenon in the variation of temperature and applied magnetic field.

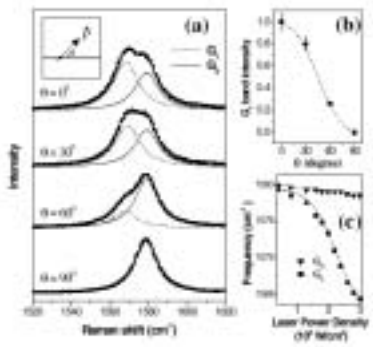

Figure 1. (a) Raman spectra obtained for light incident with different polarization angles (θ) with respect to the ribbon direction. The inset shows a schematic figure of the sample (horizontal gray line) showing the direction between the ribbon axis and the light polarization vector ($\vec{P}$). (b) Intensity of the G_1 peak versus . The dotted line is a cos2θ theoretical curve. The error bars are associated with baseline corrections. (c) Raman frequencies of the G_2 (triangles) and G_1 (squares) peaks as a function of the laser power density.

IV-D-18 Anisotropy of the Raman Spectra of Nanographite Ribbons

CANÇADO, L. G.[1]; PIMENTA, M. A.[1]; NEVES, B. R. A.[1]; MEDEIROS-RIBEIRO, G.[2]; ENOKI, Toshiaki[3]; KOBAYASHI, Yousuke[4]; TAKAI, Kazuyuki[4]; FUKUI, Ken-ichi[4]; DRESSELHAUS, M. S.[5]; SAITO, Riichiro[6]; JORIO, A.[1]
([1]Univ. Federal Minas Gerais; [2]Laboratório Nacinal Luz Síncrontro ; [3]IMS and Tokyo Inst. Tech.; [4]Tokyo Inst. Tech.; [5]MIT; [6]Tohoku Univ. and CREST JST)

[*Phys. Rev. Lett.* **93**, 047403 (4 pages) (2004)]

A polarized Raman study of nanographite ribbons on a highly oriented pyrolytic graphite substrate is reported. The Raman peak of the nanographite ribbons exhibits an intensity dependence on the light polarization direction relative to the nanographite ribbon axis. This result is due to the quantum confinement of the electrons in the 1D band structure of the nanographite ribbons, combined with the anisotropy of the light absorption in 2D graphite, in agreement with theoretical predictions.

IV-E Molecular Crystals toward Nano-Devices by Use of *d*-π Interaction, Crystal Designing and Optical Doping

After some 30 years' intensive research on molecular charge transfer (CT) salts as potential functional materials, the research field has now gotten ready to examine how to make them into actual devices. Such efforts are concentrated on the developments of organic thin films for field effect transistors and light-emitting devices, both of which are carried out in a number of laboratories and groups with worldwide competitions. In order to examine the potential applicability of molecular materials from a different point of view, we are carrying out basic studies on development and physical properties of molecular CT single crystals. Major part of our study can be classified into three categories; the physical properties of the CT salts including localized spins, crystal designing using poly-carboxylate anions, and device formation by optical doping method.

IV-E-1 Light-Induced Transformation of Molecular Materials into Devices

NAITO, Toshio; INABE, Tamotsu[1]; NIIMI, Hironobu[1]; ASAKURA, Kiyotaka[1]
([1]Hokkaido Univ.)

[*Adv. Mater.* in press]

Many kinds of molecular solids are now attracting a worldwide interest as promising candidates for advanced materials such as electronic/magnetic/optical devices and energy converters. In particular, semiconductor diodes based on photovoltaic effect appear one of the most effective ways to utilize molecular materials, if there is an appropriate doping method available. This work concerns a finding of a novel method of (persistent) carrier doping to molecular materials. The method is simple and versatile; just illuminating the desired part of material as long as it contains a photosensitive chemical species in addition to an electroactive one. Although various kinds of photo-excited states reported thus far have typical lifetimes of some hundreds of micro-seconds at longest in general, the doped state survived even several months after the illumination was finished. The experimental results demonstrate that one can control the conducting properties of an arbitrary part of a molecular material using appropriately focussed illumination. In other words, this method opens a new way for making devices and conducting nano-architectures from a wide variety of molecular solids, which have awaited for a space-resolved doping method under a mild condition.

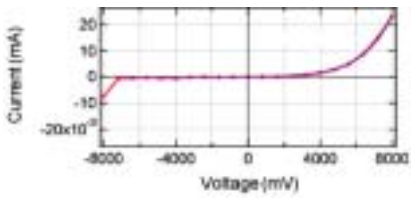

Figure 1. Current-Voltage property curve of the single crystal of $Ag(DM)_2$ after UV-VIS illumination upon only half of it for ~ 21 days.

IV-E-2 Molecular Conductors Containing Photoreactive Species

NAITO, Toshio; INABE, Tamotsu[1]
([1]Hokkaido Univ.)

[*J. Phys. IV France* **114**, 553–555 (2004)]

In order to examine the possibility of (persistent) carrier doping to molecular crystals by light exposure, some different types of molecular crystals containing photoreactive species are synthesized and characterized. The $[Ru(bpy)_3]^{2+}$ cation (bpy = 2,2'-bipyridyl) yielded two different new complexes with $[Ni(dmit)_2]^{-}$ radical species, both of which were structurally characterized and turned out to be band insulators. Methy viologen (MV) has been found to yield a new phase of the complex with $[Ni(dmit)_2]^{-}$, $MV[Ni(dmit)_2]_2$. The temperature dependences of electrical resistivity (decreasing with lowering temperature down to 1.0 K) and magnetic susceptibility (Pauli paramagnetism from 300 K to 1.8 K with a hysteresis below ~ 100 K) clearly indicate that this phase is metallic. The thermoelectric power exhibited ~ 0 μVK^{-1} from 300 K–4.2 K. This phase turned out to be metastable, and the crystals gradually turned into insulating ones. The effects of UV-VIS light exposure to the conducting and magnetic properties of $Ag(DMe\text{-}DCNQI)_2$ have been studied, and clear differences between the exposed and the pristine crystals were observed. The ESR signal at 3.7 K suggested that the exposed sample should include the Ag(0) species.

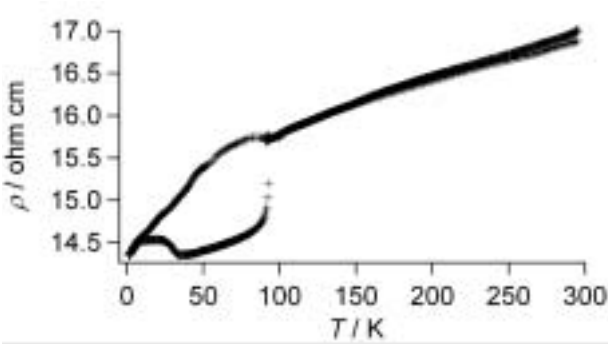

Figure 1. Temperature-dependent electrical resistivity of $MV[Ni(dmit)_2]_2$.

IV-E-3 Molecular Unit Based on Metal Phthalocyanine Designed for Molecular Electronics

MATSUDA, Masaki[1]; HANASAKI, Noriaki[1];

IKEDA, Shingo[1]; TAJIMA, Hiroyuki[1]; NAITO, Toshio; INABE, Tamotsu[2]
([1]Univ. Tokyo; [2]Hokkaido Univ.)

[*J. Phys. IV France* **114**, 541–543 (2004)]

We obtained three conducting crystals based on a $[Fe^{III}(Pc)(CN)_2]$ molecular unit. All crystals showed a large anisotropic negative magnetoresistance arising from the π-*d* interaction self-contained in the $[Fe^{III}(Pc)(CN)_2]$ unit. The anisotropy is attributable to the anisotropic *g*-tensor in the $[Fe^{III}(Pc)(CN)_2]$ unit. We also obtained a thin film containing $[Fe^{II}(Pc)(CN)_2]$. The film exhibits photocurrent response for the UV irradiation. These features suggest $[M(Pc)(CN)_2]$ molecular unit is a well-designed one for a building block of molecular devices.

IV-E-4 Anisotropic Giant Magnetoresistance Originating from the π-*d* Interaction in a Molecule

MATSUDA, Masaki[1]; HANASAKI, Noriaki[1]; TAJIMA, Hiroyuki[1]; NAITO, Toshio; INABE, Tamotsu[2]
([1]Univ. Tokyo; [2]Hokkaido Univ.)

[*J. Phys. Chem. Solids* **65**, 749–752 (2004)]

We synthesized $TPP[Fe^{III}(Pc)(CN)_2]_2$, $PTMA_x[Fe^{III}(Pc)(CN)_2]{\cdot}y(MeCN)$, and $PXX[Fe^{III}(Pc)(CN)_2]$, a new series of charge-transfer salts containing the axially-substituted phthalocyanine (Pc), $[Fe^{III}(Pc)(CN)_2]^-$. In this molecular unit, the π conduction electron derived from the Pc-ring coexists with the *d* electron which is a potential source of a local magnetic moment. Therefore various phenomena associated with the interplay between local magnetic moments and conduction electrons are expected. We observed the giant negative magnetoresistance (GNMR) in all the three salts. The GNMR is highly anisotropic for the magnetic-field direction, and reflects the *g*-tensor anisotropy of the local magnetic moment in the $[Fe^{III}(Pc)(CN)_2]^-$ unit. This indicates that the GNMR in these salts originates from the strong π-*d* interaction in the $[Fe^{III}(Pc)(CN)_2]^-$ unit.

IV-E-5 Novel Phthalocyanine Conductor Containing Two-dimensional Pc Stacks, $[PXX]_2[Co(Pc)(CN)_2]$ (PXX = *peri*-Xanthenoxanthene, $Co(Pc)(CN)_2$ = Dicyano(phthalocyaninato)cobalt(III))

ASARI, Takehiro[1]; NAITO, Toshio; INABE, Tamotsu[1]; MATSUDA, Masaki[2]; TAJIMA, Hiroyuki[2]
([1]Hokkaido Univ.; [2]Univ. Tokyo)

[*Chem. Lett.* **33**, 128–129 (2004)]

A novel phthalocyanine conductor containing 2-D–stacks of the partially oxidized $Co(Pc)(CN)_2$ units has been obtained by the electrochemical oxidation method with PXX. The crystal is highly conductive (> 10^3 Scm^{-1}) at all the temperatures measured (5 K < *T* < 300 K). Though the metallic character becomes clearer compared with the single chain or ladder chain conductors, the 2-D sheet has been found to be still anisotropic.

IV-E-6 Contribution of Degenerate Molecular Orbitals to Molecular Orbital Angular Momentum in Molecular Magnet $Fe(Pc)(CN)_2$

HANASAKI, Noriaki[1]; MATSUDA, Masaki[1]; TAJIMA, Hiroyuki[1]; NAITO, Toshio; INABE, Tamotsu[2]
([1]Univ. Tokyo; [2]Hokkaido Univ.)

[*J. Phys. Soc. Jpn.* **72**, 3226–3230 (2003)]

We measured the static magnetic susceptibility and the electron spin resonance of the $Fe(Pc)(CN)_2$ complexes, and investigated the molecular magnetism of the unit $Fe(Pc)(CN)_2$. The magnetic susceptibility shows a highly anisotropic Curie behavior. Based on the electron spin resonance, we found a highly anisotropic *g*-value (g_1 = 3.62, g_2 = 1.11, and g_3 = 0.52) in the molecular unit $Fe(Pc)(CN)_2$. This anisotropy is caused by the molecular orbital angular momentum in the degenerate next highest occupied molecular orbitals of the molecular unit $Fe(Pc)(CN)_2$. Since the molecular unit $Fe(Pc)(CN)_2$ has a unique structure with fourfold symmetry, the molecular orbital angular momentum has a finite value of $l_z \sim +1$ and –1. The anisotropic molecular magnetism of the unit $Fe(Pc)(CN)_2$ contributes the highly anisotropic Curie behavior. The molecular unit $Fe(Pc)(CN)_2$ is a good candidate for a molecular magnet having high magnetic anisotropy.

IV-E-7 Angle-Resolved Mapping of the Fermi Velocity in a Quasi-Two-Dimensional Organic Conductor

KOVALEV, A. E.[1]; HILL, S.[1]; KAWANO, Koichi[2]; TAMURA, Masafumi[2]; NAITO, Toshio; KOBAYASHI, Hayao
([1]Univ. Florida; [2]Toho Univ.)

[*Phys. Rev. Lett.* **91**, 216402 (2003)]

We demonstrate a new method for determining the Fermi velocity in quasi-two-dimensional (Q2D) conductors. Application of a magnetic field parallel to the conducting layers results in periodic open orbit quasiparticle trajectories along the Q2D Fermi surface. Averaging of this motion over the Fermi surface leads to a resonance in the interlayer microwave conductivity. The resonance frequency is simply related to the extremal value of the Fermi velocity perpendicular to the applied field. Thus, angle dependent microwave studies enable a complete mapping of the in-plane Fermi velocity. We illustrate the applicability of this method for the highly 2D organic conductor κ-$(BEDT\text{-}TTF)_2I_3$.

IV-E-8 Molecular Hexagonal Perovskite: A New Type of Organic-Inorganic Hybrid Conductor

NAITO, Toshio; INABE, Tamotsu[1]

([1]Hokkaido Univ.)

[*J. Solid State Chem.* **176**, 243–249 (2003)]

An organic charge-transfer (CT) salt $(BEDT\text{-}TTF)_3(MnCl_3)_2(C_2H_5OH)_2$ has been synthesized by a standard electrochemical method. The crystal data are monoclinic, *C*2/*c* (#15), a = 38.863(4) Å, b = 6.716(1) Å, c = 23.608(3) Å, β = 115.007(3)°, V = 5584(1) Å^3, and Z = 4. The structure consists of one-dimensional (1D) infinite $\{[MnCl_3]^-\}_\infty$ magnetic chains and two-dimensional (2D) organic conduction pathways. The former consists of face-sharing octahedra of manganese chloride complex ions, and dominates the magnetic properties of this compound. Such a feature of the crystal structure closely relates to transition metal hexagonal perovskite compounds, all of which are known for frustrated triangular lattices comprised of weakly interacting 1D magnetic chains. The new compound exhibits a high conductivity down to 4 K.

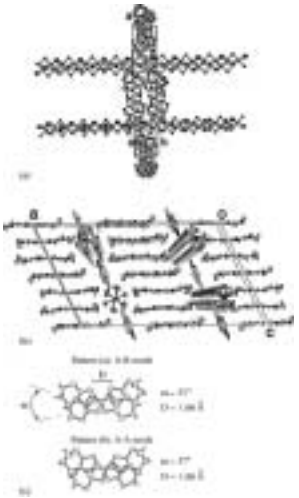

Figure 1. (a) Unit cell viewed down along the *c*-axis and (b) viewed down along the *b*-axis. (c) Two molecular overlapping modes of ET. Hydrogen atoms are omitted for clarity except in (c).

IV-E-9 Structure and Physical Properties of Low-Dimensional Molecular Conductors, $[PXX][Fe^{III}(Pc)(CN)_2]$ and $[PXX][Co^{III}(Pc)(CN)_2]$ (PXX = *peri*-Xanthenoxanthene, Pc = Phthalocyaninato)

MATSUDA, Masaki[1]; ASARI, Takehiro[2]; NAITO, Toshio; INABE, Tamotsu[2]; HANASAKI, Noriaki[1]; TAJIMA, Hiroyuki[1]
([1]Univ. Tokyo; [2]Hokkaido Univ.)

[*Bull. Chem. Soc. Jpn.* **76**, 1935–1940 (2003)]

A novel low-dimensional molecular conductor, $[PXX][Fe^{III}(Pc)(CN)_2]$, has been synthesized. This salt contains the magnetic Fe^{III} ion (S = 1/2), and is isomorphous with $[PXX][Co^{III}(Pc)(CN)_2]$ which includes the non-magnetic Co^{III} ion. In both salts, the $[Mc(Pc)(CN)_2]$ (M = Fe or Co) units form a two-leg ladder chain. The two salts exhibit a similar temperature dependence of the thermoelectric power and a similar reflectance spectrum. The Fe^{III} salt shows semiconducting behavior in its electrical resistivity over the temperature range measured, while the isomorphous Co^{III} salt exhibits metallic behavior in its resistivity above 100 K. The difference in the transport properties between the two salts suggests that the conduction electrons in the Fe^{III} salt are seriously scattered by the local magnetic moment. Spontaneous magnetization is observed below 8 K in the Fe^{III} salt. Upon applying a magnetic field, the resistivity of the Fe^{III} salt drastically decreases below 50 K. The decrease in the resistivity is highly anisotropic to the field orientation. The field orientation dependence is highly consistent with the *g*-tensor anisotropy in the $[Fe^{III}(Pc)(CN)_2]$ unit, suggesting that the negative magnetoresistance originates from the large π-*d* interaction self-contained in the $[Fe^{III}(Pc)(CN)_2]$ unit.

IV-E-10 Torque Study of $TPP[Fe(Pc)(CN)_2]_2$ (TPP = Tetraphenyl Phosphonium and Pc = Phthalocyanine)

HANASAKI, Noriaki[1]; MATSUDA, Masaki[1]; TAJIMA, Hiroyuki[1]; NAITO, Toshio; INABE, Tamotsu[2]
([1]Univ. Tokyo; [2]Hokkaido Univ.)

[*Synth. Met.* **137**, 1227–1228 (2003)]

The magnetic torque shows the anomaly around 20 K. The torque curve suggests the antiferromagnetic state in the one-dimensional $Fe(Pc)(CN)_2$ chain. The magnetic easy axis is directed along the CN-ligand in the $Fe(Pc)(CN)_2$ unit. Because of the strong spin-orbit coupling, the next highest occupied molecular orbital is also ordered so that the molecular orbital angular momentum of the neighboring $Fe(Pc)(CN)_2$ unit is antiparallel. We observed the weak ferromagnetism below 6 K. This is ascribed to the canting of the antiparallel moments.

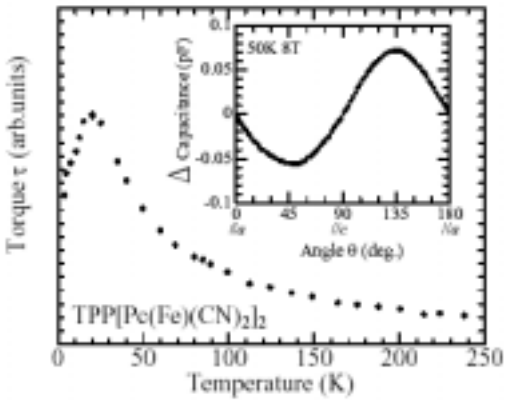

Figure 1. Temperature dependence of the torque. Inset: Torque curve measured under the magnetic field rotated within the *ac* plane.

IV-E-11 Physical Properties of $(ET)_3(MnCl_4)(TCE)$ and the Related Salts

NAITO, Toshio; INABE, Tamotsu[1];

AKUTAGAWA, Tomoyuki[1]; HASEGAWA, Tatsuo[1]; NAKAMURA, Takayoshi[1]; HOSOKOSHI, Yuko; INOUE, Katsuya
([1]Hokkaido Univ.)

[*Synth. Met.* **135-136**, 613–614 (2003)]

The ET salt with a magnetic counter ion $(ET)_3(MnCl_4)(TCE)$ (TCE = 1,1,2-trichloroethane) exhibits pressure-sensitive, complicated electrical behavior due to its semimetallic electronic structure. On the other hand, stronger d-π coupling is suggested in $(ET)_3(MnCl_3)_2(C_2H_5OH)_2$, which has infinite magnetic chains with semimetallic conducting behavior.

IV-E-12 Magnetic Properties of *d*-π Conducting System, TPP[$Fe^{III}_xCo^{III}_{1-x}$(Pc)$(CN)_2]_2$

MATSUDA, Masaki[1]; HANASAKI, Noriaki[1]; TAJIMA, Hiroyuki[1]; SAKAI, Fumiko[1]; NAITO, Toshio; INABE, Tamotsu[2]
([1]Univ. Tokyo; [2]Hokkaido Univ.)

[*Synth. Met.* **135-136**, 635–636 (2003)]

We have studied the magnetic susceptibility for one-dimensional system, TPP[$Fe^{III}_xCo^{III}_{1-x}$(Pc)$(CN)_2]_2$ ($0.07 \le x \le 1$). At $x = 1$, the system shows anisotropic Curie-Weiss behavior and spontaneous magnetization below 6 K. The temperature below which spontaneous magnetization occurs (T_c) shifts downward with a decrease in Fe^{III} concentration, but is still above 2 K at $x = 0.07$. The anisotropic Curie-Weiss behavior in the susceptibility was observed for all the alloys measured. This magnetic anisotropy was associated with the g-tensor anisotropy in the [Fe^{III}(Pc)$(CN)_2$] unit.

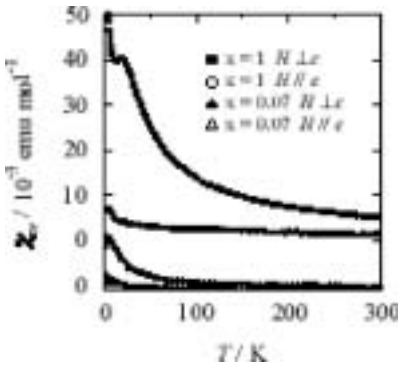

Figure 1. Temperature dependence of the magnetic susceptibility for aligned crystals of TPP[$Fe^{III}_xCo^{III}_{1-x}$(Pc)$(CN)_2]_2$ ($x = 1$ and 0.07). The magnetic field was applied perpendicular and parallel to the c-axis. Note the 1×10^{-3} emu mol^{-1} offset for $x = 0.07$.

IV-E-13 Magnetic and Optical Properties of One-Dimensional π-*d* System with Axially Substituted Iron(III) Phthalocyanine

MATSUDA, Masaki[1]; HANASAKI, Noriaki[1]; TAJIMA, Hiroyuki[1]; NAITO, Toshio; INABE, Tamotsu[2]
([1]Univ.Tokyo; [2]Hokkaido Univ.)

[*Synth. Met.* **133-134**, 547–548 (2003)]

We have measured the angular dependence of the ESR spectra on DMDP[$Fe^{III}_{0.01}Co^{III}_{0.99}(Pc)(CN)_2$] (DMDP = dimethyldiphenylphosphonium, Pc = phthalocyanine), which is the alloy system of magnetic Fe^{III} and non-magnetic Co^{III}. The spectra exhibit giant anisotropic shift in g-value of iron(III). We also report the temperature dependence of the polarized reflectance spectra of one-dimensional conductors, TPP[Fe^{III}(Pc)$(CN)_2]_2$ and TPP[Co^{III}(Pc)$(CN)_2]_2$ (TPP = tetraphenylphosphonium). With lowering the temperature, the plasma edge drastically shifts to a higher wavenumber, and additional dispersion appears around 1600 cm^{-1} and around 3600 cm^{-1} in both salts.

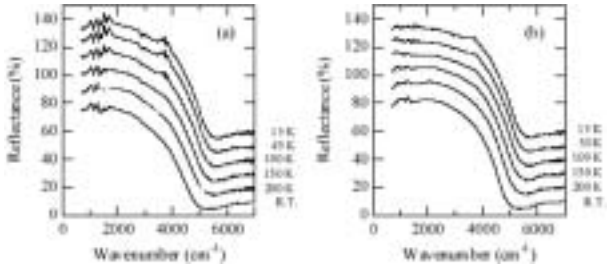

Figure 1. Temperature dependence of the reflectance spectra of TPP[Fe^{III}(Pc)$(CN)_2]_2$ (a) and TPP[Co^{III}(Pc)$(CN)_2]_2$ (b) for the polarized light parallel to the c-axis. In TPP[M^{III}(Pc)$(CN)_2]_2$, [M^{III}(Pc)$(CN)_2$] units form a one-dimensional regular chain along the c-axis. The 0% level is successively shifted by 10% for clarity.

IV-E-14 One-Dimensional π-*d* Electron System inTPP[Fe(Pc)$(CN)_2]_2$, [PXX][Fe(Pc)$(CN)_2$], and $(PTMA)_x$[Fe(Pc)$(CN)_2]_y(CH_3CN)$: Electron Spin Resonance and Negative Magnetoresistance

HANASAKI, Noriaki[1]; MATSUDA, Masaki[1]; TAJIMA, Hiroyuki[1]; NAITO, Toshio; INABE, Tamotsu[2]
([1]Univ. Tokyo; [2]Hokkaido Univ.)

[*Synth. Met.* **133-134**, 519–521 (2003)]

We measured the electron spin resonance and the magnetoresistance in the iron(III) phthalocyanine complexes. The electron spin resonance in PNP[Fe(Pc)$(CN)_2$] reveals the large anisotropy of the g-value. This is due to the strong spin-orbit coupling in the second HOMO (the third HOMO) hybridizing the d_{yz} (d_{zx}) orbital in the central Fe atom. This anisotropic g-value is consistent with the anisotropy of the magnetic susceptibility and the negative magnetoresistance in TPP[Fe(Pc)$(CN)_2]_2$. We also measured the large negative magnetoresistance in [PXX][Fe(Pc)$(CN)_2$] and $(PTMA)_x$[Fe(Pc)$(CN)_2]_Y(CH_3CN)$. The iron(III) phthalocyanine complexes are the good materials for the research of the one-dimensional π-*d* electron system.

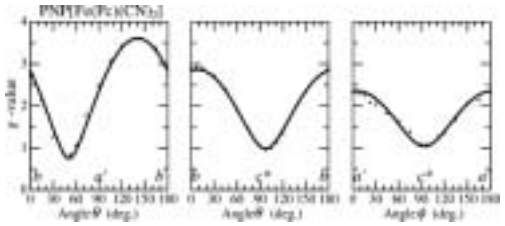

Figure 1. Angular dependence of electron spin resonance in PNP[Fe(Pc)$(CN)_2$].

IV-E-15 Phthalocyanine-Based Multi-Dimensional Conductors

INABE, Tamotsu[1]; ASARI, Takehiro[1]; HASEGAWA, Hiroyuki[1]; MATSUDA, Masaki[1]; GACHO, Eduardo H.[1]; MATSUMURA, Naoko[1]; TAKEDA, Sayaka[1]; TAKEDA, Keiji[1]; NAITO, Toshio
([1]Hokkaido Univ.)

[*Synth. Met.* **133-134**, 515–518 (2003)]

Electrochemical oxidation of $[Co^{III}(Pc)X_2]^-$ yields highly conducting partially oxidized salt crystals. Their crystal structures and dimensionality of the π-π interaction (electronic system) vary by the cationic species in the salts; one-dimensional for TPP (tetraphenylphosphonium) or PTMA (phenyltrimethylammonium) cations, and ladder and two-dimensional for the PXX (*peri*-xanthenoxanthene) radical cation. Substitution of the axial group (X) or extension of the π-conjugated macrocycle (Pc) has been found to influence the magnitude of the π-π stacking interactions. Their electrical properties characterized by the conductivity and thermoelectric power measurements are found to be dependent on the dimensionality and the magnitude of π-π stacking interactions.

IV-E-16 $ET_3(MnCl_3)_2(EtOH)_2$: A New Organic Conductor with A Perovskite Structure

NAITO, Toshio; INABE, Tamotsu[1]; AKUTAGAWA, Tomoyuki[1]; HASEGAWA, Tatsuo[1]; NAKAMURA, Takayoshi[1]
([1]Hokkaido Univ.)

[*Synth. Met.* **133-134**, 445–447 (2003)]

The title salt was obtained as fine black needles from the electrolysis of ET (ET: bis(ethylenedithio)tetrathiafulvalene) with a Mn cluster in 1,1,2-trichloroethane containing 10% of ethanol. The conductivity at room temperature was 25 S cm^{-1} with weakly semiconducting behavior, yet the salt kept a high conductivity down to 4 K (~ 0.1 S cm^{-1}). The manganese(II) chloride anion formed an infinite chain made of face-shared $MnCl_6$ octahedrons, and these chains formed insulating sheets with ethanol molecules between the chains. The ET cation radicals formed α-type conducting sheets between the insulating sheets. Such crystal structure was characterized as that of a typical hexagonal perovskite ABX_3, where A equals to a bulky monocation. The magnetic behavior was reproduced by the Curie-Weiss law, which might be attributable to the face-shared $MnCl_6$ octahedron chains.

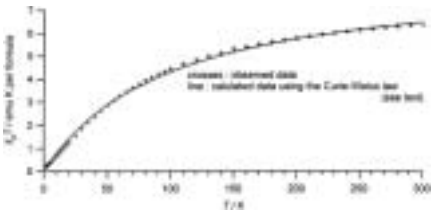

Figure 1. Temperature dependence of the magnetic susceptibility of $(ET)_3(MnCl_3)_2(C_2H_5OH)_2$.

IV-E-17 Hydrogen-Bond Networks of Mellitate Anions ($[C_6(COO)_6H_{6-n}]^{n-}$) in Salts with Pyridine Derivatives

KOBAYASHI, Norihito[1]; NAITO, Toshio; INABE, Tamotsu[1]
([1]Hokkaido Univ.)

[*Bull. Chem. Soc. Jpn.* **76**, 1351–1362 (2003)]

Single crystals of mellitate anion ($[C_6(COO)_6H_{6-n}]^{n-}$) salts with 3-aminopyridinium, $[3\text{-}NH_2C_5H_4NH^+]_3[C_6(COO)_6H_3^{3-}]$ (**1**), 4-methylpyridinium, $[4\text{-}CH_3C_5H_4NH^+]_2[CH_3C_5H_4N]_2[C_6(COO)_6H_4^{2-}]$ (**2**), $[4\text{-}CH_3C_5H_4NH^+]_2[C_6(COO)_6H_4^{2-}]\cdot 2CH_3OH$ (**3**), pyridinium, $[C_5H_5NH^+]_2[C_6(COO)_6H_4^{2-}]\cdot 2H_2O$ (**4**), 3-methylpyridinium, $[3\text{-}CH_3C_5H_4NH^+]_2[C_6(COO)_6H_4^{2-}]$ (**5**), $[3\text{-}CH_3C_5H_4NH^+]_5[C_6(COO)_6H_3^{3-}][C_6(COO)_6H_4^{2-}]\cdot CH_3OH$ (**6**), and isoquinolinium, $[C_9H_7NH^+]_2[C_6(COO)_6H_4^{2-}]\cdot CH_3OH$ (**7**), $[C_9H_7NH^+]_2[C_9H_7NH_{0.5}^{0.5+}][C_6(COO)_6H_{3.5}^{2.5-}]\cdot CH_3OH$ (**8**) have been structurally characterized. In these crystals, strong hydrogen-bonds between the mellitate anions are formed. Various arrangements that depend on the deprotonation number, *n*, have been found. All hydrogen-bonds found between the anions are combinations of a carboxy and a carboxylato group. The "triangular hydrogen-bond" unit between the anions, in which three anions are connected by the three hydrogen-bonds to form a triangle, in the salt with $n = 3$, induces the two dimensional (2-D) sheet self-organizing structure in this crystal. "Dual hydrogen-bond" units between the anions, in which two pairs of the hydrogen-bonds connect the neighboring anions, have been found in the salts with $n = 2$ or 2.5. The repetition of the co-planer "dual hydrogen-bond" induces the anion one-dimensional (1-D) belt structure, while the combination of the standing and co-planer "dual hydrogen-bond" units induces the 2-D grid structure. These 2-D grids are further linked by hydrogen-bonds to form a channel. In all the salts ($n = 3$, 2, 2.5), the counter cation molecules are arranged in the space defined by the anion network.

IV-E-18 Crystal Design of Cation-Radical Salts Based on the Supramolecular Self-Organizing Arrangement of Mellitate Anions

INABE, Tamotsu[1]; KOBAYASHI, Norihito[1]; NAITO, Toshio
([1]Hokkaido Univ.)

[*J. Phys. IV France* **114**, 449–453 (2004)]

Mellitate anions form hydrogen-bonding infinite networks in the salts with pyridinium cations. The network pattern depends on the number of deprotonation (n) from the mellitic acid; for n = 3, triangular hydrogen-bond units form a two-dimensional sheet, while for n = 2, dual hydrogen-bond units induce one-dimensional belts or two-dimensional grids. These self-organizing properties have been utilized for the crystal design of the TTF-type radical cation salts. Crystallization with TMTTF gave two kinds of crystals. One of the radical cation salt crystals consists of channel network of the anions and one-dimensional columns of TMTTF in the channels. In the other TMTTF salt, the anions with n = 1 form a two-dimensional sheet with methanol molecules. The TMTTF radicals are packed between the sheets with their molecular planes parallel to the anion planes.

IV-E-19 Network Formation of Mellitate Anions ($[C_6(COO)_6H_{6-n}]^{n-}$) in the Salts with Piperidinium Derivatives and *o*-Phenylenediammonium

KOBAYASHI, Norihito[1]; INABE, Tamotsu[1]; NAITO, Toshio
([1]Hokkaido Univ.)

[*CrystEngComm* **6**, 189–196 (2004)]

Single crystals of mellitate anion ($[C_6(COO)_6H_{6-n}]^{n-}$) with piperidinium $[C_5H_{10}NH_2^+]_3[C_6(COO)_6H_3^{3-}]$ (**1**) and $[C_5H_{10}NH_2^+]_2[C_6(COO)_6H_4^{2-}]\cdot CH_3OH\cdot 3H_2O$ (**2**), with 1-methylpiperidinium $[C_5H_{10}NHCH_3^+]_2[C_6(COO)_6H_4^{2-}]\cdot 2H_2O$ (**3**), and with *o*-phenylenediammonium $[C_6H_4(NH_3)_2^{2+}]_2[C_6(COO)_6H_2^{4+}]\cdot 2CH_3OH$ (**4**) have been prepared and structurally characterized. In all of the salts, two-dimensional (2D) networks of mellitate anions were formed due to the strong self-organization of the anion. In **1**, a 2D hexagon-type network of hydrogen-bond has been observed to form among the anions. This is characteristic of the mellitate anions with n = 3 (n: deprotonation number from the acid). In other salts, a 2D anion network containing either water molecules or $-NH_3$ groups commonly formed. Since the network pattern occurs with different cation species, this hydrogen-bonding unit was determined to be dominant in the n = 2 anion with water and the n = 4 anion with $-NH_3$ species.

IV-E-20 Physical Properties of Electrically Conducting and Stable Molecular Neutral Radical Solid $[Co(2,3\text{-}Nc)(CN)_2]CH_3CN$ (2,3-Nc = 2,3-Naphthalocyanine)

NAITO, Toshio; MATSUMURA, Naoko[1]; INABE, Tamotsu[1]; MATSUDA, Masaki[2]; TAJIMA, Hiroyuki[2]
([1]Hokkaido Univ.; [2]Univ. Tokyo)

[*J. Porphyrins. Phthalocyanines.* in press]

Solid state properties of dicyano(2,3-naphthalocyaninato)cobalt(III) neutral radical crystal, $[Co(2,3\text{-}Nc)(CN)_2]CH_3CN$, were characterized by the measurements of the resistivity under high pressure and under uniaxial strain, thermoelectric power, magnetic susceptibility, ESR and polarized reflectance spectra. The title compound exhibited thermally activated-type electrical conductivity along the *c*-axis. The room temperature (RT) resistivity ρ_{RT} along the *c*-axis and activation energy E_a rapidly decreased with increasing pressure. The temperature-dependent thermoelectric power S was that of a typical one-dimensional (1D) semiconductor. However the high absolute value of S suggested that this electronic system should be strongly correlated. Although the electrical resistivity exhibited monotonical temeperature-dependence, the magnetic susceptibility clearly indicated a Peierls-type transition and marked fluctuation from RT. Both of Peierls-type transitions and fluctuations are characteristic phenomena to 1D conductors. Furthermore ESR spectra manifested that the Peierls-type transition occurred at 100 K. The inconsistency between the electrical behaviour (without a phase-transition) and magnetic behaviour (with a phase-transition) indicates the separation of the degrees of freedom in spin and charge (spin-charge separation) of this material. Spin-charge separation is a theoretically predicted phenomenon peculiar to the 1D conductors with strong correlation. The reflectance spectra were quantitatively explained by a 1D Hubbard model, and manifested the existence of a structural fluctuation of this material from RT. Based on these observed physical properties it is concluded that $[Co(2,3\text{-}Nc)(CN)_2]CH_3CN$ is a strongly correlated 1D semiconductor with a Mott-Hubbard type energy gap and characterised with a fluctuation and spin-charge separation.

IV-E-21 Structural, Electrical and Magnetic Properties of α-$(ET)_7[MnCl_4]_2\cdot(1,1,2\text{-}C_2H_3Cl_3)_2$ (ET = bis(ethylenedithio)tetrathiafulvalene)

NAITO, Toshio; INABE, Tamotsu[1]
([1]Hokkaido Univ.)

[*Bull. Chem. Soc. Jpn.* in press]

A new charge-transfer salt of ET with a chloromanganate(II) complex anion has been synthesized and characterized by X-ray structural analysis, resistivity measurements, magnetic susceptibility, electron spin resonance (ESR) and extended Hückel tight biding band calculation. The crystal has a sheet structure comprised of α-type two-dimensional (2D) donor arrangement in the *bc*-plane and insulating sheets of discrete $[MnCl_4]^{2-}$ anions and $1,1,2\text{-}C_2H_3Cl_3$ (TCE) molecules. Its conducting property exhibits considerable anisotropy, which is of effectively metallic along the *b*-axis down to 1.2 K under 2.9 kbar and higher pressure. The magnetic susceptibility is approximately reproduced by the Curie-Weiss law with the Weiss temperature $\theta = -(1.35 \pm 0.07)$ K from 2–300 K. ESR measurements revealed that the π-electron system in this salt exhibits Pauli paramagnetism at least at 3.6– ~ 50 K. The band calculation suggests that the HOMO (the highest occupied molecular orbital) band has extremely small dispersion almost solely along the b^*-axis with a simple one-

dimensional (1D) Fermi surface. Considering all the data above, it is concluded that this salt has unusually stable and narrow 1D metallic band structure, which is a rare example even in a great number of molecular conducting salts reported to date.

IV-E-22 New Binuclear Copper Complexes $[(9S3)Cu(CN)Cu(9S3)]X_n$ (X = BF_4, *n* = 1; X = TCNQ, *n* = 2) (9S3 = 1,4,7-trithiacyclononane): Syntheses, Crystal Structures and Magnetic Properties

NAITO, Toshio; NISHIBE, Kunimasa[1]; INABE, Tamotsu[1]
([1]Hokkaido Univ.)

[*Bull. Chem. Soc. Jpn.* in press]

The binuclear Cu complexes of 1,4,7-trithiacyclononane (9S3) with an inorganic anion (BF_4^-) and with an organic radical anion $TCNQ^-$ (7,7',8,8'-tetracyanoquinodimethanide) were synthesized and their molecular and crystal structures were examined in connection with each magnetic property. A new complex cation [Cu(9S3)CN(9S3)Cu] varied its charges and magnetic properties depending on the counter anions; [Cu(9S3)CN(9S3)Cu](BF_4) (**1**) was obtained as diamagnetic colorless crystals, while [Cu(9S3)CN(9S3)Cu]$(TCNQ)_2$ (**2**) was obtained as dark blue crystals with antiferromagnetic property. Complex **1** crystallized in the monoclinic space group *C*2/*c* with *a* = 26.863(2), *b* = 7.0878(5), *c* = 13.4864(8) Å, β = 116.318(2)°. Complex **2** crystallized in the triclinic space group $P\bar{1}$ with *a* = 12.521(1), *b* = 20.2698(8), *c* = 8.0205(4) Å, α = 100.688(4), β = 93.846(5), γ = 94.953(4)°. Both complexes were comprised of cyano-bridged two Cu(9S3) ions with tetrahedral coordination geometry. The X-ray structural study revealed that **1** had two crystallographically equivalent Cu(I) centers, while **2** had two crystallographically independent Cu(I/II) sites. The two Cu(I/II) sites could not be distinguished from the X-ray structural study. As for **2** the IR spectra showed that both crystallographically independent TCNQ species were monoanions and were strongly dimerized due to pstacking, which well explained their diamagnetic contribution to the magnetic susceptibility and the highly insulating property of this salt. The temperature-dependent magnetic susceptibility of **2** showed a deviation from the Curie-Weiss behavior around 60 K, which indicated a strong antiferromagnetic intermolecular interaction between the copper complexes and that such intermolecular interaction should partly occur *via* the TCNQ radical anion dimer.

IV-E-23 Charge Disproportionation and Anomalous Giant Magnetoresistance in a One-Dimensional Conductor, $TPP[Co(Pc)(CN)_2]_2$

TAJIMA, Hiroyuki[1]; HANASAKI, Noriaki[1]; MASUDA, Kouki[1]; MATSUDA, Masaki[1]; KODAMA, Katsuaki[1]; TAKIGAWA, Masashi[1]; OHMICHI, Eiji[1]; OSADA, Toshihito[1]; NAITO, Toshio; INABE, Tamotsu[2]; HASEGAWA, Hiroyuki[3]
([1]Univ. Tokyo; [2]Hokkaido Univ.; [3]NICT)

[*Synth. Met.* in press]

Magnetoresistance study on the charge transfer salts of $[Fe(Pc)(CN)_2]$ revealed various interesting phenomena, such as anisotropic giant negative magnetoresistance, weak ferromagnetism, and anisotropic Curie-Weiss magnetic susceptivility.[1)] These interesting phenomena originate from the orbital magnetic moment remaining in the $[Fe(Pc)(CN)_2]$ unit, and the *d*-π interaction inherently existing in this unit. Contrary to the $[Fe(Pc)(CN)_2]$ salts, physical properties of the $[Co(Pc)(CN)_2]$ salts have not been investigated in detail. In this paper, we report the magnetotransport and NQR studies on $TPP[Co(Pc)(CN)_2]_2$ salts. This salt is a one-dimensional conductor, where the partially oxidized $[Co(Pc)(CN)_2]$ units stack uniformly along the *c*-axis. The salt exhibits Pauli-paramagnetic susceptibility. The electrical resistivity is semiconducting with a very small activation energy less than 0.01 eV. Interestingly, this salt exhibits very large positive magnetoresistance at low-temperature ($\Delta R(8\ T)/R(0\ T) \sim 6$). Moreover, the field orientation dependence is quite small below 10 T. These facts indicate that the magnetoresistance in this salt is not an ordinary orbital effect. In order to examine the mechanism of the anomalous magnetoresistance, we have measured ^{59}Co NQR spectra. We found a sign of charge disproportionation at 1.8 K. On the basis of magnetotransport ($B < 38$ T), NQR and NMR ($B < 16$ T) measurements, we will discuss the anomalous electronic state of this salt.

Reference

1) For example see, N. Hanasaki *et al.*, *Phys. Rev. B* **62**, 5839–5842 (2000).

IV-E-24 A New Optical Doping Method toward Molecular Electronics

NAITO, Toshio; INABE, Tamotsu[1]; NIIMI, Hironobu[1]; ASAKURA, Kiyotaka[1]
([1]Hokkaido Univ.)

[*Synth. Met.* in press]

This work concerns a finding of a novel method of (persistent) carrier doping to molecular materials. The method is simple and versatile; just illuminating the material as long as it contains a photosensitive chemical species in addition to an electroactive one. Although various kinds of photo-excited states reported thus far have typical lifetimes of some hundreds of microseconds at longest in general, the doped state survived even a week after the illumination was finished. The experimental results demonstrate that one can control the conducting properties of an arbitrary part of a molecular material using appropriately focussed illumination. In other words, this method opens a new way for making devices and conducting nano-architectures from a wide variety of molecular solids, which have awaited for a space-resolved doping method.